

Received December 2, 2015, accepted December 17, 2015, date of publication January 13, 2016,
date of current version March 4, 2016.

Digital Object Identifier 10.1109/ACCESS.2016.2517926

Model-Mediated Teleoperation: Toward Stable and Transparent Teleoperation Systems

**XIAO XU, (Member, IEEE), BURAK CIZMECI, (Member, IEEE),
CLEMENS SCHUWERK, (Member, IEEE), AND ECKEHARD STEINBACH, (Fellow, IEEE)**

Chair of Media Technology, Technische Universität München, Munich 80333, Germany

Corresponding author: X. Xu (xiao.xu@tum.de)

This work was supported by the European Research Council (ERC) through the European Union's Seventh Framework Programme (FP7/2007-2013)/ERC under Grant 258941.

ABSTRACT Bilateral teleoperation systems with haptic feedback allow human users to interact with objects or perform complex tasks in remote or inaccessible environments. Communication delays in teleoperation systems jeopardize system stability and transparency, leading to degraded system performance and poor user experience. In this paper, we provide a survey of the model-mediated teleoperation (MMT) approach, which has been developed to guarantee both system stability and transparency in the presence of arbitrary communication delays. This survey focuses on two major parts: 1) the historical development of the MMT approach from the late 1980s to the present and 2) the main challenges facing the design of a reliable MMT system. Along with the discussion of the MMT challenges and the proposed solutions, a series of experiments has been conducted to compare the performance between the existing techniques and to supply data that were missing in the previous studies on the MMT approach.

INDEX TERMS Model-mediated teleoperation, tele-haptics, time-delayed teleoperation, stability and transparency, parameter estimation, haptic data reduction, model update.

I. INTRODUCTION

Remote interaction solutions such as voice or video conferencing have reached a high level of sophistication and widespread use. While the feeling of being present in a remote environment is clearly available with these systems, a complete immersion cannot be realized without the possibility of physical interaction with the remote environment. To this end, bilateral haptic teleoperation systems have been developed. These systems supply the user with multimodal sensor information concerning the remote environment while commanding a robotic system in the remote space. Haptics, as an extension of visual and auditory modalities, refer to both kinesthetic and tactile information and include position, velocity, force, torque, vibration, etc. In this paper, we use the word *haptic* to refer to kinesthetic components such as force and motion.

Using a teleoperation system with haptic feedback, the users can thus truly immerse themselves into a distant environment, i.e., modify it, and execute tasks without physically being present but with the feeling of being there. A typical teleoperation system comprises three main parts: the human operator (OP)/master system, the teleoperator (TOP)/slave system, and the communication link/network

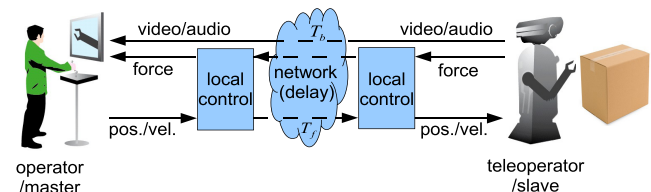


FIGURE 1. Overview of a teleoperation system (adapted from [1]).

in between [1]. During teleoperation, the slave and master devices exchange multimodal sensor information over the communication link. As illustrated in Fig. 1, the slave robot follows the received position or velocity commands sent by the master. The haptic, visual, and audio signals captured by the sensors on the slave side are sent back to the master and displayed to the OP. This teleoperation structure, sending motion (position/velocity) signals and receiving haptic signals, is referred to as position-force teleoperation architecture and is widely used [14], [15], [19]. Another teleoperation architecture relevant to this paper is the position-position structure, where the master sends its position/motion signals to the slave, and also receives the slave's position/motion signals. The haptic feedback is then

rendered based on the master and received slave motion signals [18], [41].

Use of haptic feedback, in addition to visual and audio information increases the sense of being present in the remote environment [8], thereby allowing an OP to perform dangerous tasks at a safe distance. Applications include the handling of nuclear/toxic/explosive materials [2], the exploration of space and underwater [3]–[5], and the improvement of a user's ability to perform complex tasks such as telesurgery [6] and tele-teaching/tele-training [7]–[11]. For an overview please refer to [12].

Communication between geographically distributed master and slave systems over a network is afflicted with time delay and packet loss. Communication delay normally ranges from a few milliseconds up to several hundred milliseconds, depending on distance and the communication infrastructure. The delay can even increase to several seconds in space applications. As many studies have shown, even a small communication delay or packet loss rate in the haptic channel jeopardizes the system's stability and transparency [13]. To guarantee stability and to improve the level of transparency in the presence of communication unreliabilities, passivity-based control schemes, such as the wave-variable (WV) transformation [14]–[16] (see Fig. 2(a)) or the time domain passivity approach (TDPA) [17]–[19] (see Fig. 2(b)), have been developed. Ideal system transparency is defined as a perfect match between master and slave position and force signals [20], or a match between the environment

impedance and the perceived impedance by the OP [13]. System stability (passivity) and transparency, however, are conflicting objectives in passivity-based teleoperation system design [13]. This means that the system gains stability at the cost of degraded transparency [14], [15], [19], [24], [25]. An overview of passivity-based teleoperation control schemes can be found in [21]–[23].

Model-mediated teleoperation (MMT) has been proposed to address both stability and transparency issues in the presence of communication delays [26]–[28] and packet loss [29]. In the MMT approach, a local object model is employed on the master side to approximate the slave environment. The model parameters describing the object in the slave environment are continuously estimated in real time and transmitted back to the master whenever the slave obtains a new model. On the master side, the local model is reconstructed or updated on the basis of the received model parameters, and the haptic feedback is computed on the basis of the local model without noticeable delay (see Fig. 2(c)). If the estimated model is an accurate approximation of the remote environment, both stable and transparent teleoperation can be achieved [27], [30], [31].

Figure 2 shows a comparison between the conventional passivity-based teleoperation architectures (the WV method and the TDPA, Fig. 2(a) and 2(b)) and the MMT architecture (Fig. 2(c)). In the passivity-based architectures, the control blocks (wave-variable transformation or passivity observer) ensure system passivity by dissipating system output energy by modifying the corresponding velocity and force signals. Additionally, in the TDPA architecture, the computed system energy needs to be exchanged between the master and slave. Compared to the passivity-based architectures, the MMT approach requires neither a modification of the velocity and force signals nor the exchange of information about the system energy. MMT systems do not send the delayed force signals back to the master. Instead, they generate non-delayed force feedback based on a local model on the master side which is an approximation of the remote environment. The authors of [32] compared 10 different control schemes including the passivity-based control and predictive control (an early version of MMT) in terms of their stability region, position and force tracking, displayed impedance, position drift, etc.

For the passivity-based architectures, balancing system conservatism (amount of dissipated energy) and system passivity is one of the main challenges for achieving high system transparency [13], [20]. For the MMT architecture, the challenges are quite different from the passivity-based architectures. In general, an MMT system requires a fast and accurate environment modeling method. These modeling methods include parametric and non-parametric approaches (see Sec. 3). Besides this, data communication, local model updating, and stable slave controlling are also important challenges for MMT (see Sec. 2.2). The number of studies on MMT and MMT-relevant challenges has rapidly increased in recent years due to the benefits of MMT in terms of system

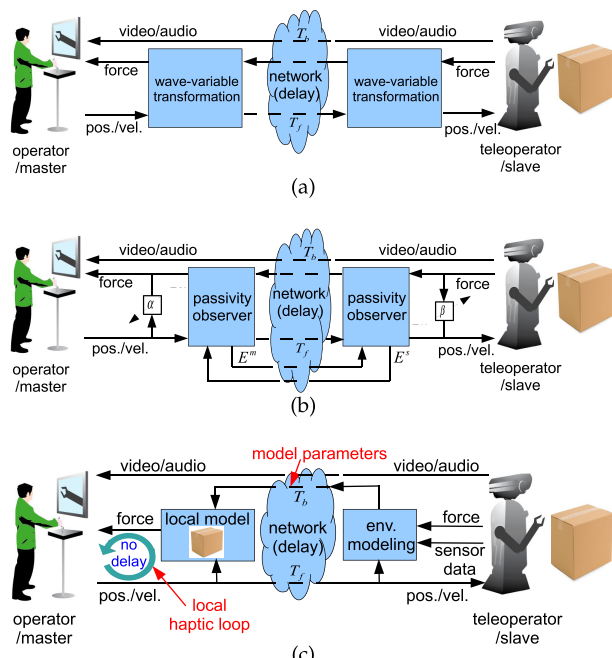


FIGURE 2. (a) Passivity-based teleoperation using the wave-variable transformation. (b) Passivity-based teleoperation using the time-domain passivity approach. For (a) and (b), the velocity and force signals are modified to guarantee system passivity. (c) A state-of-the-art model-mediated teleoperation architecture. The use of the local model enables non-delayed haptic rendering thus guaranteeing system stability.

stability and transparency. To the best of our knowledge, however, a comprehensive survey of MMT does not exist.

In this paper, we present a survey of MMT and summarize its main challenges. Studies of and corresponding solutions to these challenges are also discussed. In addition, we present a series of experiments to compare the performance between the existing techniques and to supply the data that were missing in previous studies. As the field of MMT is very broad, we do not claim this survey to be complete, but its goal is to cover and highlight the most important issues related to the MMT approach. Analytic analysis for system stability and transparency is beyond the scope of this paper. However, MMT-relevant stability and transparency issues will also be discussed.

The remainder of this paper is organized as follows. In Sec. 2, we review the development of MMT and discuss the challenges facing this technique. In Secs. 3, 4, 5, and 6, we review the corresponding studies on these challenges. System transparency of MMT is discussed in Sec. 7. Sec. 8 concludes the paper and outlines open issues for future studies.

II. DEVELOPMENT AND CHALLENGES OF MODEL-MEDIATED TELEOPERATION

MMT has been studied by a great number of researchers since the late 1980s. Different names have been suggested for the general concept of MMT. Among them, the most frequently used ones are adaptive impedance-reflecting teleoperation [26], [33], [34], [36], [38], model-based teleoperation [39], [40], model predictive/prediction-based teleoperation [41]–[44], [48], [50], virtual-reality-based teleoperation [49], and MMT [27], [28], [35], [37]. After more than 25 years of development, some challenges of MMT have already been intensively studied, while others are still lacking solutions. In the following, we briefly review the development of MMT and provide a summary of the main challenges facing MMT.

A. DEVELOPMENT OF MMT

1) ORIGINS

The key idea of MMT is to use a predicted environment model on the master side to locally provide a stable and non-delayed force feedback. The idea of environment prediction can be traced back to 1957, the year that the Smith Predictor was developed to eliminate the potential instability caused by delayed feedback signals [51]. This method, named after its inventor Otto J. M. Smith, however, was not proposed for teleoperation systems but for stabilizing a general feedback control system in the presence of time delay.

The use of prediction of the remote environment for teleoperation systems originated in the late 1980s. At that time, the so-called predictive display approach was developed to visually compensate for the communication delay [52], [53]. In [52], a computer graphics model of the slave arm was overlayed on real video images. This allowed the OP to locally view the motion of the slave robot before it

actually moved and, hence, to avoid possible collisions. An extension of this idea in [54] additionally provides the user with a photorealistic view on the remote slave using three-dimensional (3D) environment reconstruction in combination with texture-mapping. A predictive display with force feedback for teleoperation systems was presented in [40] by Kotoku. The force signals were generated based on a predefined spring-damping model.

In 1989, Hannaford [26] proposed an online environment estimation scheme for teleoperation systems, called bilateral impedance control. This concept of using an online estimated environment model to provide non-delayed force feedback signals is very similar to the state-of-the-art MMT approach. Hence, we consider the structure proposed in [26] to be the first prototype of MMT. The online estimation algorithm focused on estimating the impedance of the OP and the environment (H-matrix). As illustrated in Fig. 3, the estimator calculates the applied force/torque and the equivalent impedance at the OP port and the environment port and transmits the estimates $\hat{\theta}_{1,2}$ to the other side for position/force tracking. It was proved that if the estimates of the environment model approach their actual quantities, and if the actuator is able to represent a large impedance, then the teleoperation system can be ideal in the presence of communication delays.

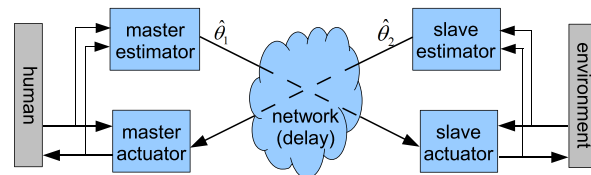


FIGURE 3. First prototype of the MMT control architecture. The exchanged parameters $\hat{\theta}_{1,2}$ contain the effort (force/torque) and impedance on both the master and slave sides (adapted from [26]).

2) SMITH PREDICTOR-BASED PREDICTIVE CONTROL

From early 2000s, predictive control was studied for stabilizing teleoperation systems with time delays [41]–[47], wherein the most typical system structure was based on the Smith Predictor.

The Smith Predictor [51] was originally designed to stabilize a linear time-invariant (LTI) system in the presence of time delays. As illustrated in Fig. 4(a), the transfer function of the example system is

$$\frac{Y}{X} = \frac{G_1 G_2 e^{-sT}}{1 + G_1 G_2 e^{-2sT}} \quad (1)$$

The delay term e^{-2sT} in the denominator indicates potential instability. The use of the Smith Predictor in Fig. 4(b) leads to a modified transfer function:

$$\frac{Y}{X} = \frac{\hat{G} G_2 e^{-sT}}{1 + \hat{G} G_2 e^{-2sT}} \quad (2)$$

where $\hat{G} = \frac{G_1}{1 + G_1 \hat{G}_2 (1 - e^{2sT})}$. If \hat{G}_2 is an accurate prediction of

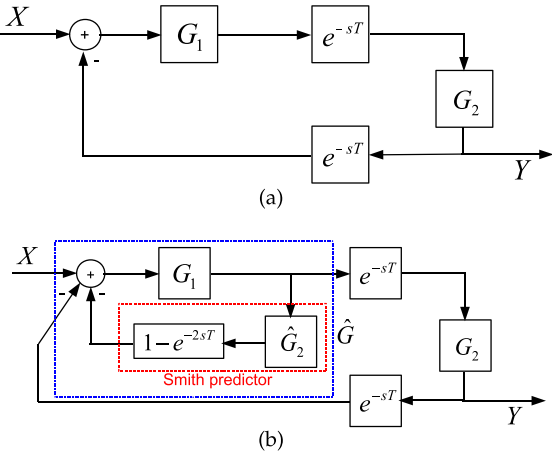


FIGURE 4. (a) An example system block diagram with delays. (b) The use of the Smith predictor to compensate for the delays (adapted from [51]).

\$G_2\$ (\$\hat{G}_2 = G_2\$), the transfer function of Fig. 4(b) becomes

$$\frac{Y}{X} = \frac{G_1 G_2 e^{-sT}}{1 + G_1 G_2} \quad (3)$$

which ensures a stable system if \$G_1\$ and \$G_2\$ are stable. Obviously, the Smith Predictor can eliminate the potential instability caused by the delayed feedback signal.

Based on the Smith Predictor, Huang and Lewis proposed a recurrent neural network (RNN)-based predictive control scheme for a position-position teleoperation architecture [41]. The proposed RNN estimator is able to model the non-linear behavior of the slave-environment system. Non-linear in this context means that no linear relationship between the system outputs (i.e. force) and the system inputs (i.e. position, velocity, and acceleration) exists. A typically and widely used non-linear environment model is the Hunt-Crossley model (see Sec. 3.1.1). On the other hand, if a linear relationship exists between the inputs and outputs, the system is linear (e.g., the Kelvin-Voigt model [71], [72]).

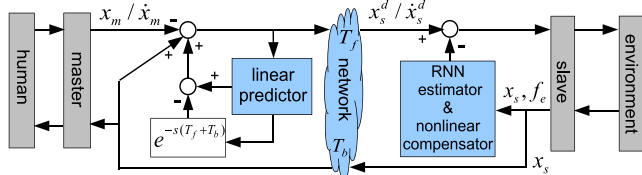


FIGURE 5. Predictive control architecture using a Smith Predictor for a position-position teleoperation system. The linear predictor on the master side is designed offline. The environment can be non-linear. Here \$x_m\$ and \$x_s^d\$ denote the master and desired slave position. \$x_s\$ and \$f_e\$ are the measured slave position and slave contact force. Adapted from [41].

As discussed in [41] and illustrated in Fig. 5, the non-linear slave-environment behavior is assumed to contain an invariant linear part, which is used on the master side to predict the slave behavior. A non-linear compensator is designed on the slave side to compensate for the model mismatch between the linear predictor on the master side and the non-linear behavior on the slave side. The assumption of an invariant

linear part in the slave-environment non-linear behavior limits the system capacity for dealing with time-varying slave-environment behavior, since the linear predictor on the master side is predefined and not updated in real time. However, for teleoperation with rich knowledge about the remote environments (e.g., pre-scanning and available history data for the current environment), a precisely predefined environment model can also provide stable haptic interaction without the need for parameter estimation. The idea of using predefined models has been adopted for many applications, such as predictive aid in teleoperation systems [40], [55], in-orbit space robot teleoperation [39], and MMT systems with pre-scan process [56]. The use of predefined models in MMT systems shows some level of improved stability against communication delay, and also of robustness against small modeling errors [39].

A consequence of using a predefined model is obviously the potential modeling error. This error originates from the difficulty of modeling complex environments and the limited resolution of the sensor measurements. In practice, there are situations in which we have limited knowledge about the remote environment, especially when the slave enters a new environment or interacts with dynamic (movable or deformable) objects. Therefore, online environment modeling and model updating are inevitable. This requires the slave system to be able to extract the environment geometry and impedance in real time. The geometry represents the position and shape of the object model, while the impedance describes the physical properties of the environment model, including mass/inertia, stiffness/compliance, damping, friction, etc.

The authors of [46] and [47] discussed the Smith predictor-based predictive control structures which allowed for an online environment modeling method. Fite et al. proposed a model-based prediction in [45] to enable a teleoperation system to deal with a time-varying environment. The environment is assumed to be a linear spring model, and the model parameter (stiffness) is continuously estimated and updated online on both the master and slave sides. In [42] and [43], a neural network (NN)-based prediction scheme for dealing with both non-linear and time-varying environments has been developed. As illustrated in Fig. 6, the NN estimator is trained online to model the environment input-output dynamics. The trained weights of the NN estimator \$\mathbf{W}_{ji}\$ are transmitted back to the master to update the local NN model. If the estimation is accurate, the estimated force \$\hat{f}_e\$ on the master side with

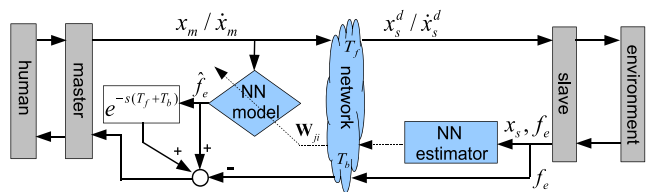


FIGURE 6. Predictive control architecture using a Smith Predictor for a position-force teleoperation system with the force feedback term. Adapted from [42] and [43].

the delay term $e^{-s(T_f + T_b)}$ is able to cancel the received (and delayed) slave contact force f_e . Note that although the transmitted weights are delayed, they converge to stable values and have minimal changes after the initial learning period is passed.

This scheme retains the original structure of the Smith Predictor. The communication delay, however, must be known to eliminate the effect of the delayed force signal on the master side. In addition, imprecise modeling of the environment leads to incomplete cancellation of the contact force from the slave side, and results in potential contact oscillation and control difficulties. Alfi et al. proposed a modified structure in [47] to improve system robustness against uncertainties of time delay and model parameters. In the presence of measurement errors in time delay and model parameters, simulation results showed good performance of their method in motion and force tracking. To completely avoid these issues, the authors of [42] and [43] presented a zero-feedback NN-based predictive control scheme, where the slave force is no longer sent back to the master (Fig. 7). The force signal on the master side is only computed based on the local NN-model. Thus, knowing the communication delay is not required. Improvements on system performance while using the zero-feedback structure are shown in [42] and [43]. However, the system stability of this control architecture highly depends on the accuracy of the environment model and the employed schemes for model updating on the master side.

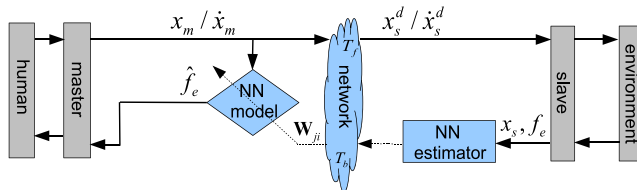


FIGURE 7. Predictive control architecture using a Smith Predictor for a position-force teleoperation system without force feedback term. Adapted from [42] and [43].

The capability of dealing with nonlinear and varying environments in the presence of unknown communication delay enables the zero-feedback predictive control scheme to serve as a benchmark for studies of the MMT approach. In fact, the general structure in Fig. 7 is conceptually identical to the state-of-the-art MMT architecture illustrated in Fig. 2(c). We use the architecture illustrated in Fig. 2(c) to represent an MMT system in the following, if no further specification is made.

3) MMT IN COMPLEX ENVIRONMENTS

The Smith Predictor-based studies on MMT introduced in Sec. II-A.2 mainly focus on 1D environments without modeling the environment geometry. From the year 2000 onward, studies on MMT have turned to the matter of efficiently modeling complex environments, including their impedance and geometry in 3D space, and how to stably update the local model on the master side and stably control the slave system

when the local model and the environment mismatch. In fact, model mismatch can lead to a mismatch in position tracking on the slave side, resulting in dangerous slave behavior such as undesirably deep penetration into an object or improperly large force acting on the environment (see Sec. VI).

Mitra and Niemeyer were the first to use the name MMT in [27] to indicate an alternative type of information exchange between the master and slave. Different from the conventional teleoperation architecture wherein the force signals are transmitted in the backward channel, MMT systems send the estimated model parameters back to the master. The authors also presented a qualitative analysis of the trade-off between the level of communication delay and the level of abstraction in control schemes. They suggested that the abstraction for control schemes should adapt to the communication delay in order to maintain successful teleoperation. As illustrated in Fig. 8, the MMT approach according to this analysis is able to deal with relatively larger communication delays. The relatively lower update rate of MMT implies that the MMT approach is unsuitable for quickly changing environments, since frequent updating of the model parameters could lead to stability issues. In [27], a constrained model update scheme on the master side and a position-force-switching control scheme on the slave side are proposed to avoid instability when the slave is first establishing an environment model or a model update is needed. A general discussion of the system stability of MMT can be found in [57].

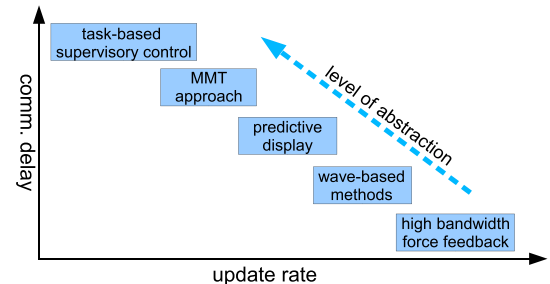


FIGURE 8. The level of abstraction and data complexity with update rates and robustness to delays (adapted from [27]).

For MMT with an unknown environment geometry, Tzafestas et al. in [33], Verschueren et al. in [58], and Xu et al. in [59] proposed online estimation algorithms for 1D, 2D, and 3D environment models, respectively. These algorithms use the position and force signals measured on the slave side to estimate the environment geometry and impedance. The geometry and impedance parameters, however, can be estimated only after the slave's first contact with the environment.

Using additional sensors, e.g., a laser range finder ([50] for a 1D environment), a stereo camera ([28] for a 2D environment), or a time-of-flight camera ([60], [61] for a 3D environment), the environment geometry can be estimated even prior to contact. Prior knowledge of the environment geometry minimizes the modeling error at the time of the slave's first contact with the environment,

and improves system stability when the slave establishes a hard contact with rigid objects. A point-cloud-based MMT (pcb-MMT) system [60], [61] enables the MMT approach to deal with arbitrarily complex environment geometries. To limit the data rate which is used for updating the environment model, a perception-based data transmission and compression scheme for updating the model parameters was proposed in [61]. As illustrated in Fig. 9, the depth images captured by a 3D sensor are used to estimate the environment geometry. The corresponding impedance parameters are estimated after the slave comes into contact with the environment. They are transmitted to the master side according to the adaptive updating scheme once the model parameters are obtained. On the master side, a local model is reconstructed based on the received model parameters (environment impedance and point cloud data). Thus, the force feedback signal can be generated locally without noticeable delays. The environment modeling, perceptual data transmission, and local haptic rendering were integrated into a pcb-MMT framework in [61].

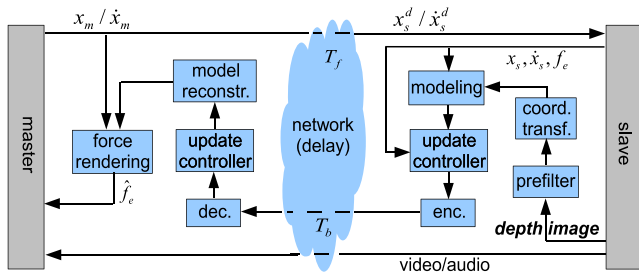


FIGURE 9. Overview of a point-cloud-based model-mediated teleoperation system using additional 3D sensors (adapted from [61]).

B. CHALLENGES OF MMT

Environment modeling is the foremost challenge in MMT, since a perfect match between the local model and the environment enables stable teleoperation in the presence of arbitrary communication delays. If the models of the master and the slave environment are mismatched (which happens normally due to environment changes, improper model approximation, or inefficient parameter estimation methods), a model update on the master side is required. According to whether the local model matches the remote environment, we define the following two states for MMT:

- **Steady state:** The estimated model parameters have converged to the actual quantities, and the local model on the master side matches the environment. Model updates in this state are not required. For an efficient MMT system, the teleoperation system should be in steady state as often and as long as possible.
- **Transition state:** Due to environment changes or inaccurate environment estimation, a model mismatch between the local model and the actual environment may occur. In this case, the local model needs to be updated as quickly as possible. Transition states occur irregularly during teleoperation.

Beside online model estimation, handling the stability issues in a transition state is another important challenge for MMT. An analysis of the MMT control block helps us understand the concrete issues related to this challenge. First, we modify the MMT structure that is illustrated in Fig. 2(c) to the control block diagram in Fig. 10. The estimated environment parameters are denoted as $\hat{\theta}$.

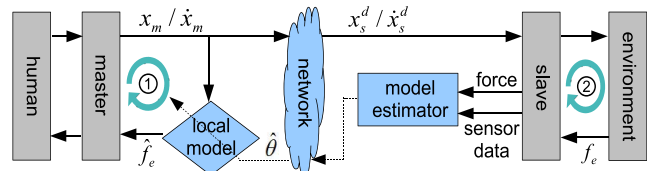


FIGURE 10. Overview of an MMT control architecture without force transmission in the backward channel.

Unlike the conventional teleoperation architecture, the MMT approach opens the control loop between the master and slave and leads to two decoupled control loops, one on the master and one on the slave side as illustrated in Fig. 10. The stability of the MMT system can be determined using the stability of the human-master local model closed loop (loop 1) and the slave-environment closed loop (loop 2), which has been discussed in [30], [31], and [77]. During the transition state, the geometry and impedance of the local model could dramatically change, resulting in unstable haptic rendering in loop 1. Meanwhile, due to the model mismatch in the transition state, the master could use an improperly large force signal to command the slave or could command the slave to access an unreachable position, e.g., deep penetration of a rigid object. This could lead to the damage of both the slave robot and the objects in the remote environment. Thus, a stable haptic rendering (model updating) approach and a stable slave control scheme in a transition state are required. We consider this to be another important challenge facing MMT.

In addition, attention must be paid to data transmission in the communication network. First, network resources and transmission conditions limit the update rate of the model parameters. Second, the potential loss of the packets that contain environment parameter updates may introduce additional model mismatch. Both these increase the time period of the transition state and can lead to aggravated stability issues. Thus, it is necessary to design an efficient and reliable communication protocol for transmitting model parameters to achieve a stable MMT system.

According to the discussion above, we summarize the main challenges of MMT.

- 1) A stable and quickly convergent parameter estimation method for a model that approximates the environment on the slave side, discussed in Sec. III.
- 2) An efficient and reliable data transmission for model parameters over the network, discussed in Sec. IV.
- 3) A stable haptic rendering algorithm, based on the local model, with changing model parameters on the master side, discussed in Sec. V.

- 4) A stable slave control scheme for safe position and force tracking on the slave side during the period of model mismatch, discussed in Sec. VI.

We observe that all these challenges except the first one directly deal with the issues in transition states. However, this does not mean that the MMT system is absolutely stable in steady state without any constraints. In fact, the haptic rendering (loop 1 in Fig. 10) suffers from various stability issues in the steady state. For instance, stability of haptic rendering in the steady state is influenced by environment stiffness, damping, and sampling period [62]–[65]. In addition, the slave-environment interaction (loop 2 in Fig. 10) in the steady state can also be unstable, especially when the slave establishes a hard contact [66], [67]. However, these stability problems in the steady state are not particular issues for MMT but general issues for teleoperation systems. As there have already been intensive studies on these issues in teleoperation systems, we do not focus on them in this paper. Instead, we focus on the aforementioned four challenges particular to MMT systems.

Some of the studies discussed in the following sections do not focus on MMT systems directly but rather on the fields of robotic systems, haptic rendering in virtual environments, or human psychophysics. However, their methods, system design, and experimental results are very relevant to MMT and can be directly used for addressing its challenges. Therefore, we consider these studies to be *MMT-relevant* and include them in our following discussion.

III. ENVIRONMENT MODELING

The task of environment modeling is to identify the input-output response of the slave-environment system. Depending on whether environment models are known or not, the identification can be divided into parametric and non-parametric methods, respectively. In parametric methods, an environment model is assumed based on certain pre-knowledge or previously available information. The identification involves the estimation of the model parameters including the geometry and the physical properties in real time. This is referred to as *online parameter estimation* or *online contact dynamics identification*. For non-parametric methods, no assumption is made for the environment models, and the aim of the identification is to directly estimate a linear or non-linear input-output mapping for the slave-environment system.

In this section, we discuss both the parametric (Sec. 3.1) and non-parametric (Sec. 3.2) environment modeling methods. In addition, we also touch on the issues that are relevant to environment modeling such as persistent excitation and estimation limits (Sec. 3.3), and the modeling of human behavior (Sec. 3.4).

A. PARAMETRIC ENVIRONMENT MODELING

One of the earliest studies on contact dynamics identification for robotic systems is impedance control [66]. The knowledge of the slave-environment contact dynamics plays

a fundamental role in several robotics tasks and teleoperation systems. The availability of an accurate description of contact dynamics is helpful for allowing the robot controller to be adaptive to the current working conditions, e.g., the interaction with compliant or stiff environments [66], [68]. Different kinds of estimation algorithms, such as adaptive-control-based methods [38], [69] and various kinds of least squares methods [70], [71], have been developed. Most of these approaches can be used for MMT systems. However, these methods can only deal with *linear* environments without estimating environment geometry. Reviews and comparisons of these methods can be found in [71] and [72].

To avoid repeating the work presented in [71] and [72], we focus on the more recent estimation methods that are not discussed in the two review papers. The estimation approaches investigated in the following include parameter estimation for *nonlinear* models with known environment geometries and parameter estimation for linear models with geometric uncertainty. With known geometry, the initial position (or surface information) of the object model in the remote environment is assumed to be known. The geometry parameters are normally not included in the environment model. With geometry uncertainty, the position and orientation of the object model are among the parameters that need to be estimated.

1) NON-LINEAR MODEL WITH KNOWN GEOMETRY

The Hunt-Crossley model [73] shows nonlinear behavior of its contact dynamics, using a position-dependent environment damping model:

$$F(t) = \begin{cases} Kx^n(t) + Bx^n(t)\dot{x}(t) & x(t) \geq 0 \\ 0 & x(t) < 0 \end{cases} \quad (4)$$

where $x(t)$ represents the penetration of the slave end-effector, K is the stiffness, B denotes the damping, and n is a constant that typically lies between 1 and 2. Compared with the Kelvin-Voigt model (the dynamics of a linear damper-spring system), the Hunt-Crossley model is more consistent with physical intuition and the notion of a coefficient of restitution, which represents the energy loss during impacts [74]. Typical parameter estimation algorithms for the Hunt-Crossley model have been proposed in [75] and [76], referred to as the two-stage method [75] and the single-stage method [76], respectively.

a: THE TWO-STAGE METHOD

To handle the non-linearity of (4) with respect to the exponent n , the estimation of K and B is separated from the estimation of n . As illustrated in Fig. 11, two recursive least squares (RLS) estimators are designed for the two-stage method. In the first stage Γ_1 , the values of K and B are estimated by minimizing the force error between the measured slave contact force and the computed force based on the employed environment model, assuming that \hat{n} is known. In the second stage Γ_2 , the parameter n is estimated by assuming known \hat{K} and \hat{B} .

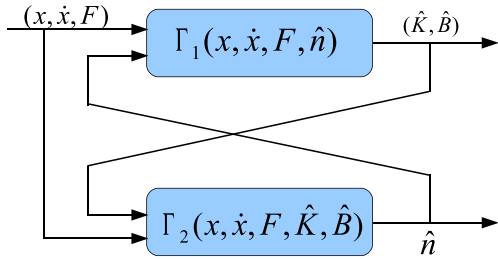


FIGURE 11. The two-stage estimation method for the Hunt-Crossley model (adopted from [75]).

Obviously, the estimation of Γ_2 is dependent on Γ_1 and vice-versa, as each estimator relies on the results from the other stage. The authors of [75] have also found that the convergence conditions for the two-stage method are very strict. First, the number of samples for estimating the model parameters must be sufficiently large. Second, the convergence is very sensitive to the initial values of $\{\hat{K}, \hat{B}, \hat{n}\}$. An improper choice of the initial values causes substantial estimation errors, resulting in slow convergence or even unstable estimation.

b: THE SINGLE-STAGE METHOD

The single-stage method [76] can estimate all three parameters K , B , and n with one RLS estimator. It also requires less restrictive conditions for convergence compared to the two-stage method.

Considering the environment model in (4), the measured slave contact force for the single-stage method can be expressed as follows:

$$F(t) = Kx^n(t) + Bx^n(t)\dot{x}(t) + \epsilon \quad (5)$$

where ϵ is the measured noise. A natural logarithm of both sides is used to decouple the parameter estimation:

$$\begin{aligned} \ln F(t) &= \ln(Kx^n(t))(1 + \frac{B\dot{x}(t)}{K} + \frac{\epsilon}{Kx^n(t)}) \\ &= \ln K + n \ln x(t) + \ln(1 + \frac{B\dot{x}(t)}{K} + \frac{\epsilon}{Kx^n(t)}) \end{aligned} \quad (6)$$

Assuming

$$|\frac{B\dot{x}(t)}{K} + \frac{\epsilon}{Kx^n(t)}| \leq |\frac{B\dot{x}(t)}{K}| + |\frac{\epsilon}{Kx^n(t)}| \ll 1 \quad (7)$$

and using $\ln(1 + \alpha) \simeq \alpha$ ($|\alpha| \ll 1$), (6) can be linearized as

$$\ln F(t) \simeq \ln K + n \ln x(t) + \frac{B\dot{x}(t)}{K} + \frac{\epsilon}{Kx^n(t)} \quad (8)$$

The above assumption requires that at least $||\dot{x}||_\infty < 0.1K/B$ and the power of the noise to be sufficiently small. The former requirement can be easily fulfilled, since the speed of operation within the contact is not high in practice and the stiffness is normally larger than the damping parameter. The latter requirement can be approached using high resolution sensors and applying filters after the measurement.

According to (8), the environment dynamics (4) can be represented for $x(t) > 0$ as

$$y = \phi^T \theta + \bar{\epsilon} \quad (9)$$

with

$$y = \ln F, \quad \phi^T = (1, \dot{x}, \ln x), \quad \theta = (\ln K, \frac{B}{K}, n)^T \quad (10)$$

The exponentially weighted RLS (EWRLS) approach [71] is employed to compute the model parameters at the sample time $t = kT$ with the sample period T :

$$\mathbf{L}_{k+1} = \frac{\mathbf{P}_k \phi_{k+1}}{\lambda + \phi_{k+1}^T \mathbf{P}_k \phi_{k+1}} \quad (11)$$

$$\mathbf{P}_{k+1} = \frac{1}{\lambda}(\mathbf{P}_k - \mathbf{L}_{k+1} \phi_{k+1}^T \mathbf{P}_k) \quad (12)$$

$$\hat{\theta}_{k+1} = \hat{\theta}_k + \mathbf{L}_{k+1} (F_{k+1} - \phi_{k+1}^T \hat{\theta}_k) \quad (13)$$

where \mathbf{P} is the covariance matrix and λ is the forgetting factor. The estimated parameters of the model \hat{K}_k , \hat{B}_k , and \hat{n}_k can be derived from $\hat{\theta}_k = (\ln \hat{K}_k, \frac{\hat{B}_k}{\hat{K}_k}, \hat{n}_k)^T$.

The sensitivity of the single-stage and two-stage methods with respect to initial conditions, parameter variations, the estimation-convergence rate, and the computational load are investigated in [76]. Compared with the two-stage method, the single-stage method is not only faster but also more robust against noise, insensitive to the initial values of the dynamic parameters, and capable of tracking finite abrupt changes in the model parameters.

One problem with using EWRLS for parameter estimation is that once the estimated parameters converge, the covariance matrix \mathbf{P} reaches a small value; thus, the estimates of $\hat{\theta}$ do not track any changes. One solution, suggested in [71] and adopted in [77], is to use the self-perturbing RLS (SPRLS) [78]. In SPRLS, the only change compared to the EWRLS is in the updating of the covariance matrix:

$$\mathbf{P}_{k+1} = \mathbf{P}_k - \mathbf{L}_{k+1} \phi_{k+1}^T \mathbf{P}_k + \beta \text{NINT}(\gamma e_{k-1}^2) \mathbf{I} \quad (14)$$

where $e_{k-1} = F_k - \phi_k^T \hat{\theta}_{k-1}$ is the estimation error in force and \mathbf{I} is an identity matrix. γ and β are predefined parameters. The function $\text{NINT}(\cdot)$ is defined as

$$\text{NINT}(x) \begin{cases} x, & \text{if } x \geq 0.5 \\ 0, & \text{else} \end{cases} \quad (15)$$

Using SPRLS, the authors of [77] extended the single-stage method to a 6-DoF case for both linear and non-linear environment models and experimentally showed a stable and quickly converging parameter estimation.

2) LINEAR MODELS WITH GEOMETRIC UNCERTAINTY

Merely estimating the environment impedance is insufficient for MMT. Environment geometry provides another constraint on motion and force feedback. The environment geometry represents the surface position and orientation of the object model on the slave side. Using the force feedback signals, “touched” and “untouched” states can be distinguished by

defining a force threshold. The position of the object can be considered at the position where the slave state changes from “untouched” to “touched”. Using additional vision or distance sensors, the environment geometry can be estimated even before the slave comes into contact with the environment. The estimation of geometry differs according to whether additional sensors are used, as will be discussed in the following three subsections.

a: WITHOUT ADDITIONAL SENSORS (1-DoF)

Without additional visual or distance sensors, the environment geometry can only be estimated based on the slave’s motion and force feedback after the contact happens.

Funda and Paul [79] proposed a teleprogramming architecture to extract the environment geometry according to the motion restriction of the slave’s primary contact point and wrist. Kinesthetic feedback is provided based on the estimated motion constraints (environment geometry). The authors of [27] proposed a contact-determination approach to estimate the position of a 1D rigid wall:

$$\begin{aligned} \text{if: } & |F_{\text{measured}}| > F_{\text{threshold}} \\ \text{then: } & \text{contact} = \text{true} \\ \text{else: } & \text{contact} = \text{false} \end{aligned} \quad (16)$$

where F_{measured} is the force measured by the sensor and $F_{\text{threshold}}$ is a threshold force determined by sensor noise and disturbances. In [28], the authors extended the estimation approach to a 2D planar surface. The surface normal was extracted by the slave’s trajectory on the surface. The estimated normal is defined as being perpendicular to the line segment connecting two (or more) points.

The above mentioned approaches estimate only the environment geometry. The environment is assumed to be rigid and its impedance is set to be the maximum value of the master or slave device. In practice, the environment can be soft or deformable. The impedance of the environment is normally unknown, necessitating an estimation approach for environment geometry in combination with its impedance.

A simple solution for such a combination is to estimate the parameters of a 1D spring model with an unknown initial position. The environment is modeled as

$$F_e = K_e \cdot (x_e - x_s) \quad (17)$$

where x_s and F_e are the slave position and force signals, respectively. The stiffness K_e and initial position x_e are unknown and need to be estimated. The aim is to minimize the force estimation error defined as

$$e_f = \hat{F}_e - F_e \quad \text{with } \hat{F}_e = \hat{K}_e \cdot (\hat{x}_e - x_s) \quad (18)$$

Although (18) is a non-linear estimation problem, it can be linearized as

$$\hat{F}_e = \hat{K}_e \cdot \hat{x}_e - \hat{K}_e \cdot x_s = [-x_s, 1] \cdot \hat{\theta} \quad (19)$$

with

$$\hat{\theta}_e = [\hat{K}_e, \hat{K}_e \hat{x}_e] = [\hat{K}_e, \hat{F}_0] \quad (20)$$

RLS methods can be adopted to compute the estimates $\hat{\theta}_e$. Yet, the estimation is not guaranteed to be stable or convergent. Therefore, the authors of [33] proposed an adaptive impedance control law to ensure the asymptotic stability of the parameter estimation. The general adaptation law is assumed to be

$$\dot{\hat{\theta}}_e = -[\gamma_1, \gamma_2]^T \cdot e_f = -[\gamma_1, \gamma_2]^T \cdot (\hat{F}_e - F_e) \quad (21)$$

where the coefficients γ_1 and γ_2 are the adaptation gains. The derivation of the Lyapunov function

$$V_e = \frac{1}{2}(\hat{\theta}_e - \theta_e)^T \cdot \Gamma_e \cdot (\hat{\theta}_e - \theta_e) \quad (22)$$

is negative definite if

$$\Gamma_e^{-1} = \begin{bmatrix} \gamma_1 & 0 \\ 0 & \gamma_2 \end{bmatrix}, \quad \text{and } \gamma_1 > 0, \quad \gamma_2 > 0 \quad (23)$$

Finally, the update scheme for the estimated environment parameters is given by

$$\begin{aligned} \dot{\hat{K}}_e &= \gamma_1 x_s (\hat{F}_e - F_e) \\ \dot{\hat{x}}_e &= \frac{\hat{F}_e - F_e}{\hat{K}_e} (-\gamma_2 - \gamma_1 x_s \hat{x}_e) \end{aligned} \quad (24)$$

Experiment 1: Since the estimation process is not shown in [33], we conduct an experiment in simulation to compare the estimation results using the impedance adaptation law (IAL) [33] and the SPRLS method.

The model parameters of (17) in our experiment are the same as those in [33]: $K_e = 200N/m$ and $x_e = -0.2m$. A sinusoidal excitation with a frequency of 0.3Hz is used as the input position signal. Measurement noise is simulated by adding Gaussian noise with zero mean and a standard deviation of $0.2N$ to the sensed force signals. In addition, the adaptation gains of the IAL method are set to be $\gamma_1 = 2000$ and $\gamma_2 = 50$. The parameters of the SPRLS method are set to be $\beta = 100$ and $\gamma = 0.5$. The estimation results using the SPRLS and IAL methods are shown in Fig. 12.

According to Fig. 12, the estimated parameters using both methods converge rapidly to the actual quantities ($\hat{K}_e \approx 200N/m$, $\hat{x}_e \approx -0.2m$). The average estimation errors of the stiffness and initial position for both methods are less than 1%. However, the SPRLS method shows a rapid response with a little overshoot in its initial stiffness estimation. We also observe that the convergence rate of the IAL method is highly dependent on the adaptation gains.

b: WITHOUT ADDITIONAL SENSORS (MULTI-DoF)

For parameter estimation in higher degree-of-freedom (DoF) environments, Verschueren et al. [58] proposed a Kalman-filter-based estimation algorithm to capture the stiffness, friction coefficient, and geometry parameters of a 2D environment model. The environment is considered to be a 2D planar surface. Thus, the geometry parameters are the position and the orientation of the plane. Due to the existing friction, the direction of the force signal could deviate from the surface normal. Therefore, the surface orientation could

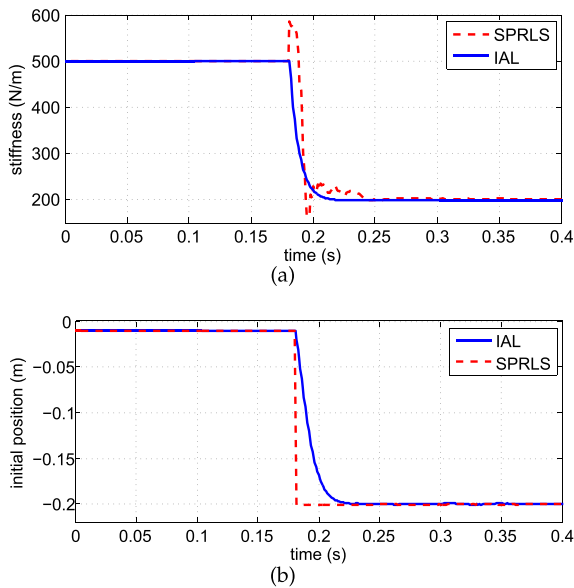


FIGURE 12. Simulation results of (a) stiffness estimation and (b) initial position estimation, using the IAL and the SPRLS methods.

not be estimated using only the force signals. However, with the help of torque signals, as proposed in [58], this issue can be addressed.

To deal with curved surfaces in 3D space, Xu et al. [59] proposed a hybrid *plane and sphere*-based algorithm to estimate the environment impedance and geometry parameters for rigid objects with complex surfaces. In [59], a plane or spherical model is adaptively employed to approximate the environments (Fig. 13). The model impedance includes only the stiffness, and the model geometry contains the position and orientation of the plane model and the position and radius for the spherical model. During the estimation process, the desired slave position (master position) is known, while the actual slave position on the surface of the rigid object is unknown.

For the plane model in 3D space,

$$ax + by + cz + d = 0 \quad (25)$$

the surface normal is described by $\mathbf{n} = [a, b, c]^T$. In the absence of surface friction, the surface normal is considered

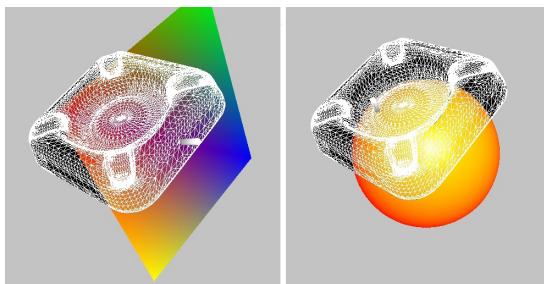


FIGURE 13. Geometric plane (left) and sphere (right) models are used to approximate the environment [59]. The model parameters are estimated based on the sampled position and force signals on the slave side.

to be identical to the direction of the measured force signal $\mathbf{f}_e = [f_x, f_y, f_z]^T$:

$$\mathbf{n} = \left(\frac{f_x}{|\mathbf{f}_e|}, \frac{f_y}{|\mathbf{f}_e|}, \frac{f_z}{|\mathbf{f}_e|} \right)^T \quad (26)$$

Thus, the geometry parameters $\{a, b, c\}$ can be computed, while the parameter d needs to be estimated. Meanwhile, the penetration depth is the shortest distance from the desired slave position $\mathbf{p}_s^d = (p_x, p_y, p_z)$ to the plane surface. With the help of Hook's law, the estimated force signal of the plane model is

$$\|\hat{\mathbf{f}}_e\| = \left(\frac{f_x p_x}{|\mathbf{f}_e|} + \frac{f_y p_y}{|\mathbf{f}_e|} + \frac{f_z p_z}{|\mathbf{f}_e|} + \hat{d} \right) \cdot \hat{K} \quad (27)$$

A linear optimization problem by minimizing the estimated force error can be established as

$$\arg \min_{\{\hat{K}, \hat{d}\}} \|\hat{\mathbf{f}}_e - \mathbf{f}_e\| \quad (28)$$

For the spherical model, the unknown impedance parameter is the stiffness, while the unknown geometry parameters are the sphere center $\mathbf{o} = (o_x, o_y, o_z)$ and its radius r . Without surface friction, the direction of the force signal is assumed to be from the sphere center to the desired slave position. The force model can be expressed as

$$\mathbf{f}_e/K = \mathbf{r} - (\mathbf{p}_s^d - \mathbf{o}) = \text{penetration} \quad (29)$$

where $\mathbf{r} = r \frac{\mathbf{f}_e}{\|\mathbf{f}_e\|}$. Eq. (29) can be expanded into a matrix-vector notation form. Replacing \mathbf{f}_e by $\hat{\mathbf{f}}_e$, \mathbf{o} by $\hat{\mathbf{o}}$, and \mathbf{r} by $\hat{\mathbf{r}} = \hat{r} \frac{\mathbf{f}_e}{\|\mathbf{f}_e\|}$, a linear optimization problem can be established

$$\arg \min_{\{\hat{K}, \hat{\mathbf{o}}, \hat{r}\}} \|\hat{\mathbf{f}}_e - \mathbf{f}_e\| \quad (30)$$

For hybrid estimation, one first applies the spherical model. If the estimated radius r is larger than a threshold value, the model is considered to be a plane, and the plane model is employed to approximate the environment. During teleoperation, the models are continuously updated to ensure a precise matching between the measured contact force and the force computed from the plane- and sphere-based model.

Note that the slave position is assumed to be unknown in this approach. In fact, the actual slave position can be also measured if the slave is equipped with position sensors. Obviously, with the help of slave position information, the model geometry can be more accurately estimated.

c: WITH ADDITIONAL SENSORS (1-DoF AND MULT-DoF)

When using additional vision or distance sensors, the estimation of the geometry parameters can be separated from the estimation of the impedance parameters. The object in the remote environment can be located before the slave comes into contact with it. The prior knowledge of the environment geometry not only provides a kinesthetic feedback before the actual contact happens, but also avoids the master commanding the slave to go to a dangerous position, e.g., deep penetration (see Sec. 6).

Using a laser rangefinder in [50], Mobasser and Hashtrudi-Zaad presented a non-contact approach for identifying environment geometry in one degree of freedom. The slave environment is approximated using a mass-spring-damper model containing the physical properties of stiffness, damping and mass. Impedance parameters (physical properties) are identified online using the SPRLS method. In addition, a collision-prediction scheme based on the information from the laser rangefinder is proposed to synchronize the collision on both the master and slave side. Similarly, Li and Song [70] fused the vision, position, and force sensor data to estimate the model position in a 1D environment.

Willaert et al. [28] extended the geometry estimation to 2D environments. A stereo camera is used to capture the position and orientation of a planar surface in the slave environment. Using a time-of-flight camera, Xu et al. [60], [61] proposed a pcb-MMT architecture (see Fig. 9), where the object surface is described by a point cloud. The captured point cloud is processed online using image inpainting filters to reduce the measurement noise and to fill holes. Thus, the pcbMMT system is able to deal with complex object geometry in 3D environments. Assuming a static and rigid environment, the stiffness and surface friction coefficient can be easily estimated based on the force signal and the known surface geometry.

Remark for Section III.A: The aforementioned parameter estimation methods are not capable of dealing with movable and deformable objects in a 3D environment. For the former, the complete model dynamics, including the object mass, friction, and free motion and rotation behaviors, are too complex to be described with a linear model [80], [81]. For the latter, surface deformation with frictional contact (sticking and sliding) on the surface is not modeled. Fortunately, there exist various methods for modeling complex deformable objects, of which multiple-degrees of freedom mass-spring models (MSM) or finite element models (FEM) are considered to be the most popular, which have been widely investigated in soft tissue simulations [82], [83]. However, online parameter estimation for MSM and FEM is quite challenging due to the computational complexity [83], [84]. The computational time needed to identify all the parameters of an FEM can range from several minutes upto several hours [84]. The challenge of online parameter estimation for deformable objects is to balance the model accuracy with the computational time.

Xu et al. proposed a radial-function-based deformation (RFBD) model in [85] to accelerate the process of online parameter estimation. The surface deformation is not dependent on complex physical models such as the MSM or FEM but is based on predefined deformation rules. As illustrated in Fig. 14 and 15, the deformation in the direction of the surface normal is approximated by a radial curve. The sticking effects due to the surface friction are described by a shearing of the radial curve in the tangential direction. In general, the RFBD method enables online parameter estimation for deformable models by means of degraded physical accuracy. However,

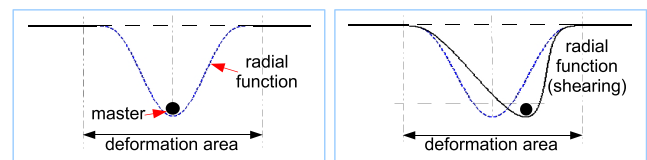


FIGURE 14. The vertical deformation of the object surface is approximated by a radial function. The tangential deformation (sticking due to the surface friction) is approximated by shearing algorithms. The blue and black lines represent the object surfaces before (left) and after (right) the corresponding tangential deformations (adapted from [85]).

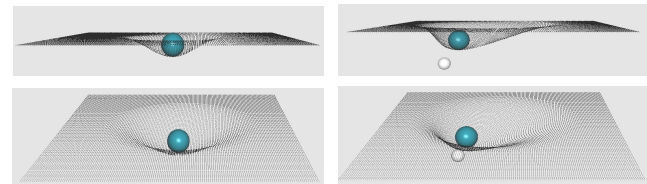


FIGURE 15. Side and top views of the surface deformation in a virtual environment. The planar surface is described by a point cloud. The blue and white spheres represent the master proxy and haptic interacting point, respectively (reproduced from [85]).

due to human perceptual tolerance, the employed model can be physically inaccurate but perceptually realistic. Future studies in this direction should focus on developing low cost and perceptually plausible models for deformable objects.

B. NON-PARAMETRIC ENVIRONMENT MODELING

The environment model can be partially or completely unknown if the slave enters an environment that is either new, has been changed, or has been previously explored, but for which historical data is not fully available (e.g., due to memory limitations). In this situation, it is difficult to employ any models to approximate the environment. Thus, parametric environment modeling is challenging. In this case, non-parametric environment modeling methods can be used. The task of non-parametric environment modeling is to directly identify the linear or nonlinear input-output mapping of the slave-environment behavior. The inputs are normally slave position, velocity and acceleration, while the output is the measured slave contact force.

To identify this non-linear mapping behavior without using an environment model, NN-based online estimation methods have been proposed [42], [43], [86]–[88]. The neuron weights are trained online to provide an accurate mapping between the slave motion (e.g. $\mathbf{x} = [x_s, \dot{x}_s, \ddot{x}_s]$) and the measured contact force f_e . Fig. 16 illustrates a NN with two hidden layers (layers 1 and 2) and a output layer (layer 3) that is used in [42] and [43]. The weight from the output of neuron i to the neuron j on layer k is denoted by $w_{i,j}^k$. The neuron in the hidden layers is composed of a sum node and a non-linear transfer function. The neuron in the output layer contains only a summation.

The main challenges of using the NN-based estimation method are the reciprocal relationships among the computational complexity, estimation accuracy, and convergence rate. Online NN-based estimation works only for a limited number

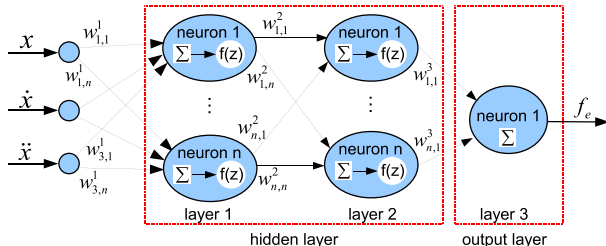


FIGURE 16. The neural network estimator used in [43]. It has three inputs, two hidden layers, and one output layer.

of hidden layers and neurons. This limitation degrades the estimation accuracy. Although it is difficult to have full information of the slave environment, having partial information of the slave environment is possible. This can come from a pre-scanning procedure or available previous knowledge of the environment. A hypothesis that needs to be verified in future work is that even for limited prior knowledge about the environment, there can be a significant improvement to the estimation accuracy of the NN estimator.

C. PERSISTENT EXCITATION AND ESTIMATION LIMITS

The concept of persistent excitation first stemmed in the 1960s [89], at which time it was generally recognized that the input signal should be persistently exciting, i.e., containing a large enough amplitude and enough different frequency components to excite all the modes of the environment model to ensure that the estimated parameters converge to their true values. For example, a non-zero velocity signal is needed to estimate environment damping, while a non-constant velocity signal is required to estimate object mass/inertia. A general framework for the discussion of persistent excitation in adaptive systems for parameter estimation can be found in [90].

Achhammer et al. [77] discuss the persistent excitation condition in MMT systems. They suggest that all the employed environment models introduced in Sec. 3.1, including the linear models and the linearized non-linear models, can be excited persistently by OPs. A rule of thumb for this is that $\lceil \frac{n}{2} \rceil$ distinct non-zero frequencies are necessary for persistently exciting a model of order n [91]. Since all the aforementioned models are of order one (after linearization) and the movements of human arm can provide at least one non-zero frequency due to its natural tremor [92], the persistent excitation is thus guaranteed if the parameter estimation process is operated by a human user.

Another important aspect of parameter estimation is the identifiable range. In [77], the authors discuss the identifiable range for stiffness. Consider a very stiff object, whose stiffness is denoted by K_e and is much larger than the slave stiffness K_s ; then, the maximum identifiable stiffness is

$$K_{max} = \frac{K_s K_e}{K_s + K_e} \simeq K_s \quad (31)$$

Therefore, the estimated stiffness is consequently limited by the slave stiffness, even with persistent excitation.

D. MODELING OF HUMAN BEHAVIOR

Just as the environment can be modeled on the slave side, human behavior can be modeled on the master side. The estimated model parameters of human behavior on the master side are transmitted to the slave to guide the slave's motion. The slave is thus not controlled by the delayed master motion commands, but performs specific tasks in complete autonomy based on the received human behavior model. Similarly, if the model as well as the model parameters can accurately approximate the user's behavior, the slave can behave like a human user and a complete skill transfer can be realized (Fig. 17) [93].

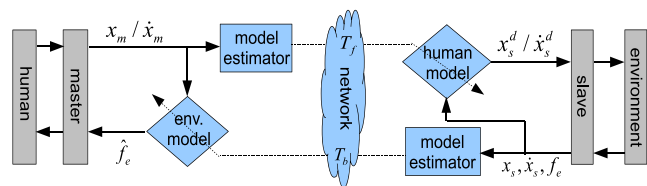


FIGURE 17. MMT system with modeling of human behavior and environment parameters (adapted from [93]).

Modeling human behavior for MMT systems has not been studied intensively so far, since human behavior is normally complicated (e.g., nonlinear) and time-varying during teleoperation. It is difficult to model such a behavior in real time. A compromise is to use fixed and predefined models to describe the motion of the human arm, and to guide the slave motion during teleoperation.

The authors of [95] presented first, second and third order predictors to estimate the position of the human arm. This method, based on the successive derivatives of the original signal, successfully compensated the effects introduced by communication delays of up to 100 ms.

In [93], the Hogan's minimum-jerk model was employed as a position assistance for slave motion. According to the Hogan's minimum-jerk model for point-to-point human arm movement [96], the current arm position x_m at time instant t can be modeled as a function of the initial position x_0 , the target position x_w , a constant impact velocity v_{hit} at the collision instant $t = T$, and the movement duration T

$$x_m(t) = x_0 + (x_w - x_0)(6\tau^5 - 15\tau^4 + 10\tau^3) + v_{hit}(-3\tau^5 + 7\tau^4 - 4\tau^3), \quad \tau = t/T \quad (32)$$

where T can be estimated in real time and the other parameters are either predefined or can be measured during teleoperation.

A non-zero impact velocity is necessary for a human user to experience the contact; however, this could destabilize the slave system at the moment of contact, especially for contact with stiff objects [97]. To overcome this issue, the authors of [93] have designed a minimum-jerk trajectory with zero impact velocity (x_r) by defining $v_{hit} = 0$:

$$x_r(t) = x_m(t, v_{hit} = 0) \quad (33)$$

The real slave trajectory x_s is a smooth transition from the human-commanded trajectory to the desired slave trajectory:

$$x_s(t) = (1 - \alpha)x_m(t) + \alpha x_r, \quad \alpha \in [0, 1] \quad (34)$$

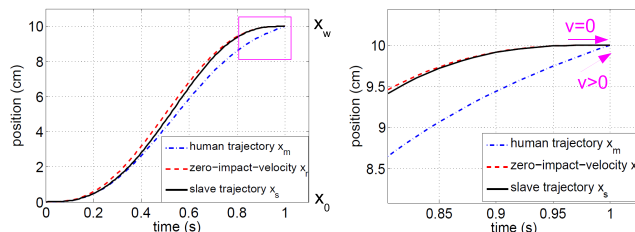


FIGURE 18. Comparison of the three trajectories of position assistance: minimum-jerk assistance, zero hit-velocity assistance, and a smooth transition between the former two. Left: full scale. Right: zoomed trajectory around x_w .

Figure 18 illustrates the three trajectories x_m (human), x_r (zero impact velocity), and x_s (slave [93]). The slave starts at x_0 along the trajectory of x_m , and smoothly transitions its trajectory to x_r during its approaching to the target position x_w . At $t = T$, the slave reaches the target position with zero velocity. The position assistance can improve system stability at the contact moment, but the realism perceived by human users is decreased [93].

Without using predefined models, the authors of [94] proposed a neuro-predictor to predict the master states such as position and force. For smooth trajectories and relatively slow movements, this method showed an improved system performance for time delays up to 1000 ms. In addition, a neural-adaptive control method presented by Li and Su [98] is able to describe human behavior and deal with input uncertainty based on the NN estimation method.

E. SUMMARY

In summary, environment modeling is the most important challenge for MMT systems. If prior knowledge about the environment is available, linear or non-linear models can be employed to approximate the environment. Various parametric methods are able to estimate the model parameters (geometry and impedance parameters) in real time during teleoperation. Without knowing the environment model, the NN-based estimation approaches (non-parametric methods) have been proposed for modeling simple environments. The accuracy and convergence of environment modeling highly depend on the persistent excitation conditions. In addition, modeling of human behavior is still underdeveloped for MMT and could be an interesting direction for future work.

IV. DATA COMMUNICATION AND DATA REDUCTION FOR MMT

For the conventional teleoperation architecture as illustrated in Fig. 1, haptic signals such as position, velocity, and force on both master and slave sides need to be sampled and

packetized immediately with a typical rate of 1 kHz. This is due to the necessity of system stability and transparency [99], [100]. Such a high packet rate together with the additional data overhead due to the transmission of packet header information leads to inefficient communication in a packet-switched network [101]. Therefore, haptic data reduction, or packet rate reduction, is required in teleoperation systems.

Haptic data reduction based on human perceptual limitations, the so-called perceptual deadband coding approach (DB approach), was introduced in [101]–[103] and [104] for conventional teleoperation systems without delay, and in [105]–[107] for systems with delay. As illustrated in Fig. 19 for a 1D example, if the change in the current signal with respect to the most recently sent signal is smaller than the perceptual threshold, the current signal will not be sent. Otherwise, the current velocity/force signal will be sent. At the receiver side, upsampling methods such as the zero-order hold (ZOH) strategy are used to interpolate the irregularly received signal samples to the high sampling rate that is required for the local control loops. The threshold is defined by considering the just noticeable difference (JND) of human perceptual discrimination for haptic signals (see Tab. 1).

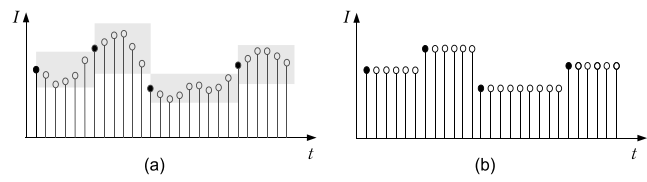


FIGURE 19. 1-Dof perceptual deadband coding approach. The input signal (a) is irregularly downsampled and only the values represented with black filled circles are transmitted. In (b), the output signal is upsampled using the zero-order-hold method (adapted from [101] and [102]).

TABLE 1. JND of human perceptual discrimination for haptic signals [25].

| Physical property | JND | Experimental conditions |
|-------------------|------------------|-------------------------|
| Force | ca. 10% | arm/forearm |
| Movement | $8\% \pm 4\%$ | arm/forearm |
| Stiffness | $23\% \pm 3\%$ | arm/forearm |
| Viscosity | $34\% \pm 5\%$ | arm/forearm |
| Inertia | $21\% \pm 3.5\%$ | pinch-fingers, at 12 kg |

For the standard MMT structure as illustrated in Fig. 10, data transmission in the forward channel is the same as that for the conventional teleoperation structure. Thus, the packet rate in the forward channel can be reduced using the state-of-the-art DB approach. In the feedback channel, the transmitted data are the model parameters instead of force signals. The transmission of the estimated model parameters can be reduced in the following two ways:

- 1) **Reduction of the estimation rate:** Model parameters are estimated only when necessary. For a slowly varying environment, there is no need to estimate the model parameters at a high rate. For example, if we estimate the environment parameters every 100ms, the packet

rate is maximally 10 packets/s. However, a too low estimation rate slows down the estimation convergence and may not be able to follow the change of the environment, even though the change is not frequent.

- 2) **Selected transmission:** This is to apply the DB approach to the estimated model parameters: not every estimate is transmitted, but only those for which the difference between the current estimate and the most recently sent estimate leads to a force feedback change at the OP larger than the JND given by Tab. 1. This scheme, in addition to the estimation rate reduction, can further reduce the packet rate in the network.

In the following, we discuss the aforementioned two data reduction methods for the standard MMT architecture.

A. ESTIMATION RATE REDUCTION

1) TIME-TRIGGERED ESTIMATION

A very simple way to reduce the estimation rate is to use a time-triggered approach. The model estimator is activated every T seconds, where T is a pre-defined estimation period. The maximum packet rate is then $\frac{1}{T}$ packets/s.

The time-triggered estimation has some drawbacks in following environment changes (e.g., stiffness change). In addition, a too large estimation period slows down the estimation convergence when the slave encounters a new environment. For the case when the slave is in contact with the environment but stops moving, signals such as the position, velocity, and force are constant. These constant signals cannot provide persistent excitation for the parameter estimation (see Sec. 3.3), resulting in invalid estimates.

2) EVENT-TRIGGERED ESTIMATION

To overcome the drawbacks of the time-triggered estimation, Verscheure et al. proposed an event-triggered estimation approach in [58]. The activation of the model estimator is not based on time but is in accordance with the slave behavior and the measured data. The rules of the event-triggered estimation can be summarized in the following three aspects:

- Estimation is activated only if the robot is moved while remaining in contact, either a normal or tangential movement.
- Geometry estimation is activated at time $T + \Delta T$ only when the slave end-effector has moved by a certain threshold amount Δs

$$x_s(T + \Delta T) - x_s(T) = \int_T^{T + \Delta T} v_s(t) dt > \Delta s \quad (35)$$

- Friction estimation is not reasonable in the sticking phase. Therefore, friction estimation is activated only when the velocity of the slave end-effector is sufficiently high ($v_s > v_{threshold}$).

Robustness of the estimation can be increased by processing the measurements only in the sliding phase, since the persistent excitation condition can be fulfilled. In addition, the estimation algorithm will not be triggered with singular

measurements such as zero velocity, thus avoiding meaningless estimation results.

B. SELECTED TRANSMISSION

Instead of sending every estimate of the environment parameters, only those estimates that result in a significant difference in perception are transmitted to the master. In the initial phase, the packet rate can be very high, since the estimates vary rapidly. Once the estimates converge to the true values, there will be no updates required and thus the system achieves zero transmission in the backward communication channel. For real teleoperation systems, however, the estimates can vary over time due to measurement noise, natural tremble of human arm movement, etc. The designed updating scheme should be robust to the parameter changes due to measurement noise and should be able to distinguish between the parameter changes due to noise and due to environment changes.

1) ENVIRONMENT IMPEDANCE UPDATE

Xu et al. proposed a perception-based update scheme in [61] to selectively transmit the estimated impedance parameters. The transmission is based on the change in the estimated physical properties. If the difference between the current estimate and the most recently sent one is larger than the JND defined by Tab. 1, an update including all the currently estimated physical properties is triggered:

$$\text{update} = \begin{cases} \text{yes,} & \text{if } \frac{Z_i(t) - Z_i(t^*)}{Z_i(t^*)} > \Delta Z_i \\ \text{no,} & \text{else} \end{cases} \quad (36)$$

where $Z_i(t)$ is the currently estimated i^{th} physical property. $Z_i(t^*)$ is the most recently triggered i^{th} physical property at time instant $t^* < t$. ΔZ_i denotes the JND of the i^{th} physical property Z_i .

Experiment 2: An experiment is conducted in simulation to evaluate the feasibility of the perception-based packet rate reduction scheme in the presence of measurement noise and environment changes. The environment is a 1D spring-damper model with an initial stiffness of 200 N/m and an initial damping of 10 Ns/m. A sinusoidal excitation with a frequency of 0.1Hz is used as the input position signal. The SPRLS method is used to estimate the impedance parameters (stiffness and damping). At time $t = 2s$, the stiffness changes to 350 N/m. At time $t = 3.5s$, the damping changes to 20 Ns/m. The perception-based updating scheme is employed to control the data transmission. The JNDs for stiffness and damping are set to be 23% and 34%, respectively, according to Tab. 1.

The simulation results are shown in Fig. 20. The estimates converge quickly at the initial contact and at the time when the environment changes. High packet rates are also observed at these time periods (see Fig. 20(c)). After the estimates converge to the true values, JNDs are not violated and thus no further updates are triggered. For infrequently varying environments, the perception-based updating scheme

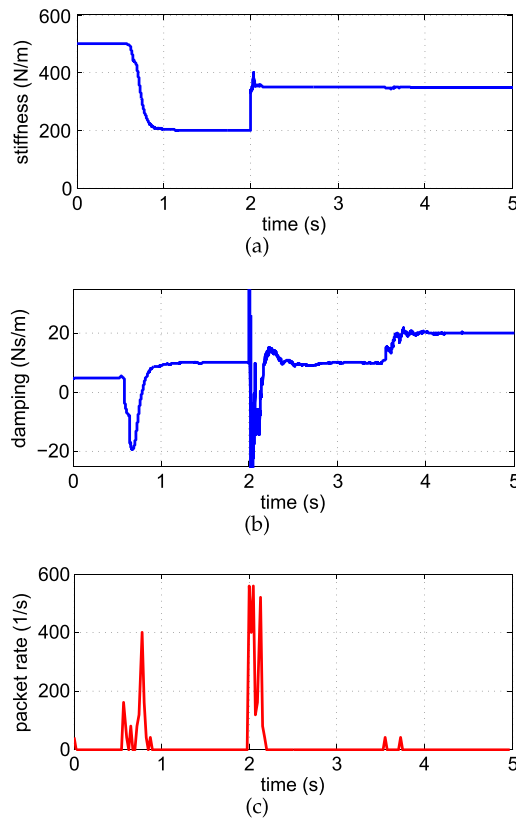


FIGURE 20. (a) Estimated stiffness values. (b) Estimated damping values. (c) Packet rate vs. time.

can achieve a high packet rate reduction, if the estimation algorithm shows fast convergence.

2) ENVIRONMENT GEOMETRY UPDATE

The geometry parameters can be updated together with the impedance parameters or they can be updated when a significant geometry mismatch, e.g., a position difference, is detected. Similar to the impedance parameters, the geometry parameters also depend on the adopted environment model. For example, if a plane model is employed, the geometry parameters are the plane normal $(a, b, c)^T$ and the plane position d (see (25)). If a spherical model is employed, the geometry parameters are the sphere center and the radius. However, a simple geometry model cannot accurately approximate complex environments. This leads to a model mismatch and results in frequent model updating (packet triggering).

To avoid frequent model mismatch in geometry parameters, the authors of [60] and [61] suggest using a point cloud to describe the complex environment geometry. The point cloud can be captured by a 3D sensor, such as a stereo camera, time-of-flight camera, and laser scanner. The update of the environment geometry is activated while the slave is in free space. It is deactivated and the impedance estimation is activated when the slave is in contact with the environment. This is to avoid sudden geometry model changes during the slave's interaction with the environment and to thus ensure a

stable exploration. The switch signal is triggered by the measured environment force. If the measured environment force is larger than a pre-defined threshold, the slave is considered to be in contact state. Otherwise, it is in free space. The captured point cloud can be easily compressed using standard image compression schemes if it is organized or using the oct-tree based compression scheme proposed in [108] if it is disorganized.

Experiment 3: In [60] and [61], point clouds are preferred over triangular meshes for two reasons. First, point-cloud-based haptic rendering, compared with mesh-based rendering [109], can provide similarly high quality haptic feedback using a simpler and faster collision detection scheme [110], [111]. In addition, if the surface point cloud is captured and streamed in real time, the use of point-cloud-based transmission and haptic rendering saves computation time for meshing and collision tree (bounding box) creation.

In this experiment, we test the time needed for meshing and bounding-box creation for a spherical model. The fast meshing algorithm proposed in [112]¹ and the axis-aligned bounding box (AABB) algorithm² are adopted for this test. This test is run on a PC with Intel(R) Core(TM) i5 CPU, 3.33GHz, 4G RAM.

TABLE 2. Computational time of meshing and bounding-box creation for a spherical model with two different resolutions.

| Dataset | points | mesh | time for meshing | time for AABB |
|----------|--------|-------|------------------|---------------|
| Sphere 1 | 4034 | 7288 | 75 ms ± 20 ms | ca. 1 ms |
| Sphere 2 | 16258 | 31652 | 400 ms ± 110 ms | ca. 30 ms |

According to Tab. 2, real-time meshing of geometry is challenging. If meshing and AABB creation are necessary for every captured point cloud frame, the maximum update rate of the point cloud is only 20 frames/s for the low resolution spherical model, and 3.3 frames/s for the high resolution spherical model. However, the resolution of a normal 3D sensor can be even higher than that of the tested model, e.g., 320×240 points in [61]. The 3D sensor captures many more points than the tested model and consequently results in more time for meshing and AABB creation. Therefore, transmitting meshes for describing environment geometry is quite difficult.

Remark for Section IV.B: An alternative way to reduce the packet rate is to apply a perceptual update scheme to the estimated force and the measured contact force. This means that if the difference between the estimated force (computed based on the estimated environment model) and the measured slave contact force is larger than the JND, an update including all the model parameters is triggered. Compared with the update scheme proposed in [61], this method requires only one JND parameter on force for the update decision. However, it is resource consuming, since the

¹Source code from pointclouds.org/documentation/tutorials/.

²Source code from www.chai3d.org.

entire force-rendering algorithm needs to be run at 1kHz on the slave side to compute the estimated force without delay. Meanwhile, the slave system has to estimate the environment parameters, which is also time-consuming if the environment is complex. Thus, to reduce the computational load on the slave side, applying JNDs directly to the estimated impedance parameters is suggested in [61].

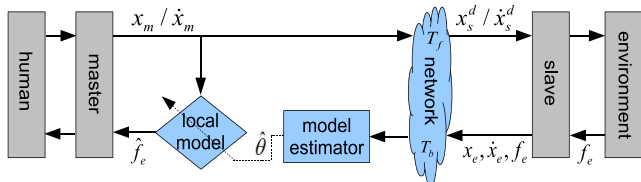


FIGURE 21. A MMT system with the model estimator on the master side.

Remark for Section IV: An alternative structure for MMT is to place the model estimator on the master side as illustrated in Fig. 21. This structure is employed in [48], [70], [93], and [96]. In this case, the only data exchanged over the network are the haptic signals, and not the environment parameters. This structure reduces the computational load on the slave side. However, for this structure it is difficult to apply the data reduction scheme. The position, velocity and force signals need to be continuously transmitted from the slave to the master, to ensure the accuracy of the online parameter estimation. Even in the case of constant contact force, signals still need to be transmitted, as a constant slave contact force does not mean that the estimation on the master side already converges. This alternative MMT structure can be used for example for ground-space teleoperation systems in which the computational capacity of the slave computer is limited by weight or cost restrictions, but communication quality is guaranteed by sufficiently high communication priority and capacity.

V. STABLE HAPTIC RENDERING

Stable haptic rendering on the master side in both transition and steady states are mandatory for the system stability of MMT. In this section, we first discuss the existing model updating schemes in the transition state. Then, we introduce the visual-haptic asynchrony issue in the steady state which could lead to potentially unstable collisions.

A. PASSIVITY-BASED MODEL UPDATING

As discussed above, the local model on the master side needs to be updated if the slave detects a new model, or if there is a significant model mismatch between the local model and the environment. In this case, the slave triggers an update. The parameters of the local model are updated according to the received data. Improper update schemes, e.g., a sudden change in stiffness or model position, result in a suddenly changed force that is displayed to the human user. This is called the model-jump effect [57]. If the users cannot adjust their arm impedance quickly enough to follow (stabilize) this

force change, an unexpected motion occurs, causing dangerous slave behavior. Therefore, smooth and stable model updating is required.

The concept of passivity is a powerful and widely used tool for the analysis of system stability, either for virtual environments [17], [62], [63] or for real teleoperation systems [15], [19]. System passivity characterizes the energy exchange over an N-port network and provides a sufficient condition for the input/output stability. Using the concept of passivity for model updating, the key point is to avoid energy injection into the system, or to ensure that the injected energy can be dissipated by system damping or friction.

1) ZERO ENERGY INJECTING

Mitra and Niemeyer have proposed a constraint-based scheme for updating model position in 1D environment to avoid energy injection [27]. For this approach, any position updating that introduces energy injection will be delayed, unless the user's motion allows for a position update that will not introduce energy injection.

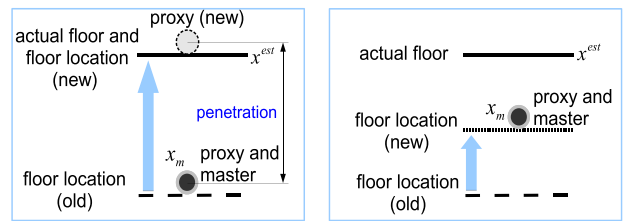


FIGURE 22. Two methods for updating object position. Left: direct updating leads to suddenly increased penetration and thus injects energy into the system. Right: gradual updating without injecting energy into the system. Adapted from [27].

As illustrated in Fig. 22, the master is in contact with the current local model (a 1D floor), while a new floor position x^{est} is detected and transmitted to the master. If the position of the floor on the master side is immediately updated to the actual position x_{est} , the penetration is increased and energy is injected into the system. This leads to a suddenly increased contact force being displayed to the user.

The solution proposed in [27] is to constrain the master floor position x_m^f to be below the master position x_m :

$$x_m^f = \min\{x^{est}, x_m\} \quad (37)$$

This means that if the master proxy moves upward, the master floor moves accordingly, but always below the proxy position. If the master moves downward, the master floor keeps still to provide a rigid contact (Fig. 22). Until the master floor reaches its actual position (the estimated position), the system switches to steady state and the constraint of (37) can be removed.

Although this updating scheme guarantees system passivity, it is designed only for position updating rather than for impedance updating. Meanwhile, the updating period can be very long, since the updating process depends on the

master's motion. Only when the master reaches the actual floor position can the entire update period be completed. In addition, Mitra et al. found that compared with some non-passive update approaches, e.g., gradually moving the master floor from the old location to the actual position at a fixed velocity, the user does not haptically prefer this passive updating scheme [113]. Therefore, further studies on the passivity-based model updating scheme are required.

2) NON-ZERO ENERGY INJECTING WITH ENERGY DISSIPATION

If the updating process leads to energy injection, but for each sampling period the same amount of energy (or more) can be dissipated, the system is still passive. According to this concept, Xu et al. [114] have proposed a passivity-based model updating scheme using adaptive damping. This approach allows for the updating of both impedance and geometry parameters in 3D environments.

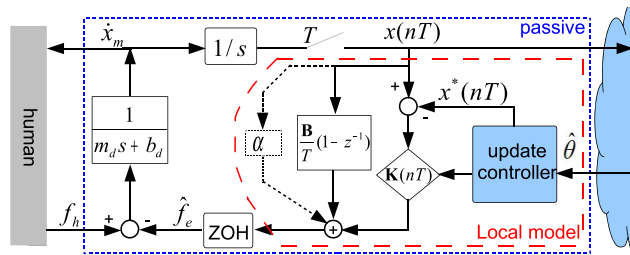


FIGURE 23. Block diagram of the master sampled-data system including a 3D spring-damper model. The unknown parameters are the stiffness, damping, and initial position of the local model (adapted from [114]).

As illustrated in Fig. 23, the environment is modeled as a spring-damper model, where $\mathbf{K} = \text{diag}(k_x, k_y, k_z)$, $\mathbf{B} = \text{diag}(b_x, b_y, b_z)$, and $\mathbf{x}^* = (x, y, z)^T$ denote the stiffness, damping, and initial position, respectively. The haptic rendering is passive if the energy storage W_s in the local model is smaller than the work input by the OP (denoted as W_h) between two samples from $t = 0$ to $t = T$. The input work W_h within a sample period T is

$$W_h = \mathbf{f}_h^T(\mathbf{x}_1 - \mathbf{x}_0) = \mathbf{f}_e^T(\mathbf{x}_1 - \mathbf{x}_0) + E_k + \int_0^T \dot{\mathbf{x}}^T \mathbf{B}_d \dot{\mathbf{x}} dt \quad (38)$$

where $E_k = \frac{1}{2}m_d(||\dot{\mathbf{x}}_1||^2 - ||\dot{\mathbf{x}}_0||^2)$ denotes the change in the kinetic energy within a sample period. $\mathbf{B}_d = b_d \mathbf{I}_3$ is the device damping. \mathbf{x}_0 and \mathbf{x}_1 are the device position vectors at the time $t_0 = 0$ and $t_1 = T$, respectively. The energy storage within a sample period T is

$$\begin{aligned} W_s &= E_k + E_e \\ &= E_k + \frac{1}{2}(\mathbf{x}_1 - \mathbf{x}_0^*)^T \mathbf{K}_0 (\mathbf{x}_1 - \mathbf{x}_0^*) \\ &\quad - \frac{1}{2}(\mathbf{x}_0 - \mathbf{x}_0^*)^T \mathbf{K}_0 (\mathbf{x}_0 - \mathbf{x}_0^*) \end{aligned} \quad (39)$$

where E_e denotes the change of the elastic potential energy within a sample period. \mathbf{x}^* is the object's initial position. \mathbf{K} is

the object stiffness matrix. The subscripts of \mathbf{K} and \mathbf{x}^* denote the corresponding time instants $t_0 = 0$ and $t_1 = T$.

Passivity conditions for updating the stiffness, damping, and initial position can be derived according to the estimated environment force $\mathbf{f}_e = \mathbf{K}_0(\mathbf{x}_0 - \mathbf{x}_0^*) + (\mathbf{B}_0 + \alpha \mathbf{I}_3)\dot{\mathbf{x}}_0$ and the constraint $W_h \geq W_s$. To simplify the passivity conditions, the authors of [114] derived a conservative condition for a 1D environment. The conclusions were as follows:

- Updating the model dampings will not break system passivity.
- Updating only the stiffness, the passivity condition is

$$\dot{k} = \frac{\Delta k}{T} \leq 2(\alpha + b_d + b - \frac{k_0 T}{2}) \cdot (\frac{\dot{x}_1}{x_1})^2 \quad (40)$$

- Updating only the initial position, the passivity condition is

$$\begin{aligned} \frac{2T\dot{x}_0}{k} [k(x_0 - x_0^*) + (b_d + b + \alpha)\dot{x}_0] + (x_0 - x_0^*)^2 \\ \geq (x_1 - x_0^* - \Delta x^*)^2 \end{aligned} \quad (41)$$

Eqs. (40) and (41) show the upper bound of the rate of change in stiffness and initial position for given dampings $[\alpha, b_d, b]$, respectively.

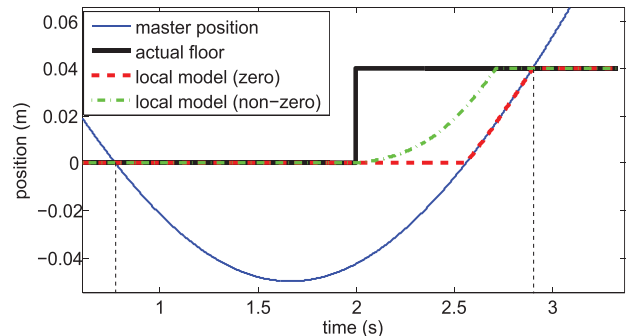


FIGURE 24. Floor position updating using the zero and non-zero energy injecting methods. Environment parameters: stiffness $k = 1000$ N/m, total system damping $b_d + b_0 + \alpha = 20$ Ns/m, and sampling time $T = 1$ ms.

Experiment 4: An experiment is conducted in simulation to compare the position updating schemes proposed in [113] and [114] for a 1D floor. As illustrated in Fig. 24, the initial floor position on the slave side (the black solid line) is at 0 m. It suddenly changes to 0.04 m at $t = 2$ s. The master (the blue solid line) is controlled so as to be in contact with and penetrate into the floor from $t \approx 0.7$ s to $t \approx 2.9$ s. After $t \approx 2.8$ s, the contact is released. During this contact, the position of the local floor model is updated in one of the two ways: 1) the zero energy injecting method [27] (the red dashed line) and 2) the non-zero energy injecting method [114] (the green dotted-dashed line).

According to Fig. 24, the non-zero energy injecting approach can update the model position faster, since the system damping can dissipate the energy generated by increasing the penetration. The updating process ends before the contact is released. The zero energy injecting method, however, only

updates the model position maximally at the current master position. Thus, the updating process is slower than the non-zero energy injecting method.

The authors of [114] also show that for stiffness updating, users prefer the non-zero energy injecting update scheme rather than the non-passive/fixed-rate update scheme proposed in [113].

B. MODEL DISPLACEMENT FOR VISUAL-HAPTIC ASYNCHRONY

In the presence of communication delay, the video signal displayed on the master side is transmitted from the slave side and thus delayed; the locally rendered force signal, on the other hand, is non-delayed. Hence, visual-haptic asynchrony (VHA) exists between the displayed video and haptic signals and increases with the communication delay. An example of this VHA effect in a 1D environment is illustrated in Fig. 25(a). At the time instant when the user haptically feels the collision, the video shows that the slave end-effector is still not in contact with the environment. For MMT systems in steady state under time delay, haptic feedback is displayed before the video signal. In this case, it is difficult for human users to predict the collision time and to control the collision velocity. An improperly large collision velocity can result in instability or cause damage to the slave robot. Therefore, the VHA effect must be properly compensated for.

The effect of VHA has been investigated in many studies including [114]–[116]. It was found that VHA could be detected by a human user when it exceeded

50ms – 150ms depending on the tasks. In addition, the VHA has negative effects on task performance and completion time. To compensate for the VHA in MMT, delaying the locally rendered haptic signal to synchronize it with the video signal is not recommended, since delayed haptic feedback leads to instability [13]. To address this issue, a dynamic model displacement scheme was proposed in [118] to compensate for the VHA while ensuring system stability. In the presence of communication delay, the position of the local model is adaptively shifted along the motion direction of the master to haptically delay the collision time (see Fig. 25(b)). With growing x_{shift} , the delay of haptic collision is increased, and thus the VHA can be reduced. While releasing the contact, the local model is gradually moved back to its actual position with the constraint on the master position, as described in [27]. The haptic signals are still rendered locally without delay; thus, the system remains stable.

The required displacement x_{shift} to fully compensate for the VHA can be computed based on the master motion and the round-trip delay T_R

$$\begin{aligned} x_{shift}(t) &= x_m(t) - x_s(t) = x_m(t) - x_m(t - T_R) \\ &= \int_{t-T_R}^t \dot{x}_m(\tau) d\tau \end{aligned} \quad (42)$$

where $x_s(t)$ is the currently displayed slave position on the delayed video, which has a delay of T_R .

With the advantage of compensating the VHA while ensuring system stability, the model displacement scheme, however, introduces two additional issues that could jeopardize system stability and transparency. First, the manual shift of the local model leads to model mismatch between the master and the slave sides. In addition, a slave control approach must be applied to guarantee a stable slave motion during the model mismatch (see Sec. 6). Second, the model displacement introduces additional movement for the human arm while establishing contact. A large x_{shift} can be perceived by the human user and leads to an unrealistic kinesthetic experience of distance. However, the reduction of x_{shift} increases the VHA. Therefore, a displacement compromise between the VHA and the perceived distance errors has been experimentally found in [118].

For example, for a constant approach velocity of 10 cm/s with a delay of 200ms, a maximum displacement of $x_{shift} = 10 \text{ cm/s} \times 200 \text{ ms} = 2 \text{ cm}$ is enough to fully compensate for the VHA. However, if the entire arm movement during the approach phase is 20 cm, the 2 cm-displacement introduces an additional 10% movement, which can be perceived by human user according to Tab. 1. Thus, we limit the displacement in this case to $x_{shift} = 1.5 \text{ cm}$. The additional movement is then less than 8% and cannot be perceived by the human user. Meanwhile, the remaining VHA is $\frac{2 \text{ cm} - 1.5 \text{ cm}}{10 \text{ cm/s}} = 50 \text{ ms}$, which could also hardly be perceived by the user. Thus, a good compromise between the VHA and subjective experience is achieved in this case.

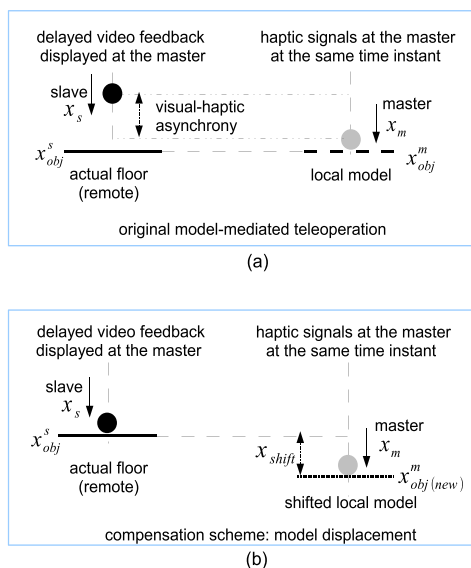


FIGURE 25. The principle of dynamic model displacement. The position of the local model is shifted downward to synchronize the haptic collision with the visual collision (adapted from [117]). x_s and x_m denote the slave and master position. x_{obj}^s and x_{obj}^m represent the position of the real object on the slave side and the position of the rendered local model on the master side, respectively. x_{shift} is the model displacement for visual-haptic synchronization.

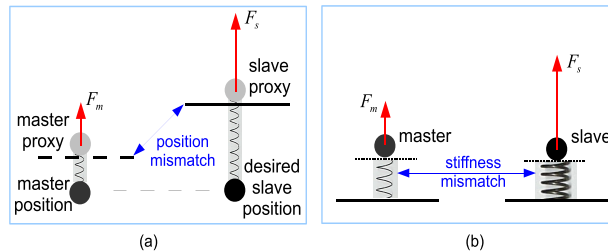


FIGURE 26. Slave control issues during model mismatch when a simple position control approach is used. (a) Position mismatch for rigid objects: undesired penetration and large contact force. (b) Stiffness mismatch for deformable objects: large contact force and improper compression.

VI. SLAVE CONTROL IN THE TRANSITION STATE

In this section, we discuss the transition-state slave control. In the transition state, the local model on the master side is mismatched to the remote environment. This model mismatch can lead to a mismatch in position tracking on the slave side, resulting in dangerous slave behavior such as undesirably deep penetration into an object or improperly large force acting on the environment (see Fig. 26). The state-of-the-art transition-state slave control approaches for dealing with such issues are the switching position control (PC)/force control (FC) method [27], [28] and the relative tracking method [61], [119]. The feasibilities of the two approaches for dealing with a position mismatch or a stiffness mismatch are discussed next.

A. SWITCHING POSITION/FORCE CONTROL

The slave is operated in PC mode if it is in free space, and is placed under FC if it is in contact with the environment. In the FC mode, the slave is controlled to execute the same task force (contact force) to the environment as applied on the master side. The switch between the two control modes is triggered by the measured environment force F_e .

$$\begin{aligned} |F_e| = 0 &\rightarrow \text{PC: } (x_s, \dot{x}_s)(t) = (x_m, \dot{x}_m)(t - T_f) \\ |F_e| > 0 &\rightarrow \text{FC: } (x_s, F_s)^{\text{task}}(t) = (x_m, F_m)^{\text{task}}(t - T_f) \end{aligned} \quad (43)$$

where T_f is the communication delay in the forward channel.

In the FC mode, the slave no longer follows the master position but applies the same task force to the environment. For the case of position mismatch, this control scheme ensures identical master and slave contact forces and prevents the slave's improper penetration into the object. However, if there is a stiffness mismatch and the stiffness of the local model is larger than that of the environment, in order to apply the same task force on both the master and slave side in the FC mode, the slave needs to compresses the environment more than on the master side. Thus, the slave reaches an improper position due to the large compression, which can lead to damages to the environment.

B. RELATIVE TRACKING

The relative tracking scheme [119] is a modification of the PD controller. The original PD controller for position tracking

on the slave side is

$$F_s = k_p(x_m - x_s) + k_d(v_m - v_s) \quad (44)$$

where F_s is the force applied to the slave and k_p and k_d are the PD gains for position and velocity. The modified PD control for relative tracking is

$$F_s = k_p[(x_m - x_w^m) - (x_s - x_w^s)] + k_d[(v_m - v_w^m) - (v_s - v_w^s)] \quad (45)$$

where x_w^m and x_w^s are the position of the local model on the master side and of the object on the slave side, respectively. v_w^m and v_w^s denote their velocities. For a static environment, $v_w^m = v_w^s = 0$.

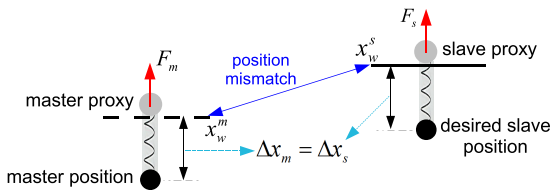


FIGURE 27. Relative tracking control scheme on the slave side for dealing with model mismatch.

The principle of the relative tracking scheme is illustrated in Fig. 27. The penetration on the slave side is identical to that on the master side. Thus, undesired penetration on the slave side can be avoided.

One problem with using the relative tracking is that when the PD gains of the slave are different from those of the master, the applied slave and master force can be different. The force deviation between the master and slave leads to potential instability.

Remark for Section VI: Using either one of the two control approaches alone cannot completely address the potential stability issues in the transition state. A solution is to use a hybrid control scheme by taking the advantage of the FC and the relative tracking approaches. This means that either when the slave contact force reaches the same quantity as the master force or when the slave penetration reaches the same depth as it does on the master side, the slave will not execute any motion commands. This stops the increase in contact force and penetration, and thus ensures stable force/position tracking on the slave side.

VII. SYSTEM TRANSPARENCY OF MMT

A comprehensive study on system transparency for MMT is not available in literature. In this section, we discuss the factors that mainly influence the transparency of MMT. In addition, we discuss a possible definition of transparency for the steady state and the transition state in MMT.

System transparency describes the accuracy with which a teleoperation system can display a remote environment to the human user. In the traditional sense, a teleoperation system is called transparent if the impedance displayed to the human user Z_h is identical to the environment impedance Z_e [13]:

$$Z_h = Z_e \quad (46)$$

This means that no external dynamics are felt in free space and that the remote environment is exactly represented on the master side during contact.

Lawrence [13] has proposed a definition for transparency error to describe the difference between the displayed impedance and the environment impedance over a certain frequency range:

$$Z_{error} = \frac{1}{\omega_{max} - \omega_{min}} \int_{\omega_{min}}^{\omega_{max}} |Z_{diff}(j\omega)| d\omega \quad (47)$$

with

$$Z_{diff}(j\omega) = |\log Z_h(j\omega)| - |\log Z_e(j\omega)| \quad (48)$$

The lower the value of Z_{error} , the higher is the degree of transparency.

For MMT systems in the steady state, system transparency depends on the accuracy of the model estimation. The estimated model impedance Z_{est} will be directly transmitted to the master and displayed to the human user. Thus, $Z_{est} = Z_h$, if no packet loss over the network is assumed. Therefore, (47) can be used to measure the steady-state transparency.

For MMT systems in the transition state, system transparency is affected mainly by the duration of the transition state. The duration T_{trans} can be defined as a sum of the round-trip delay T_R , the convergence time of the parameter estimation T_{conv} , and the duration of the model updating T_{update}

$$T_{trans} = T_R + T_{conv} + T_{update} \quad (49)$$

The smaller T_{trans} is, the shorter the transition state lasts, and thus the less model mismatch the MMT system has. Ideally, the duration of the transition state should be zero; thus, the model mismatch in the transition state is avoided. However, this is impossible due to the communication delay and the non-zero convergence time of the model estimation algorithm. The use of a quickly convergent estimation algorithm and a fast model updating scheme can improve system transparency. However, too short of an updating time leads to model jump effects and results in instability as discussed in Sec. V. From this perspective, stability and transparency become conflicting objectives.

In the transition state, the parameters of the local model are time-varying, leading to time-varying displayed impedance. Frequency analysis of the displayed impedance cannot perfectly describe the time-varying impedance. Thus, we suggest using time-frequency analysis methods such as the short-time Fourier transform (STFT). Using STFT, the displayed impedance at time t and frequency ω can be written as $Z_h(t, j\omega)$. The transparency error in the transition state is then

$$Z_{error}^{trans} = \frac{1}{\omega_{max} - \omega_{min}} \int_0^{T_{trans}} \int_{\omega_{min}}^{\omega_{max}} |Z_{diff}(t, j\omega)| d\omega dt \quad (50)$$

with

$$Z_{diff}(t, j\omega) = |\log Z_h(t, j\omega)| - |\log Z_e(t, j\omega)| \quad (51)$$

Eq. (50) indicates that longer-duration transition states cause larger transparency errors. For the ideal case where the duration T_{trans} is zero, the transparency error according to the integration in (50) is also zero. This means that zero transition duration can avoid model mismatch, which conforms to our discussion above.

The total transparency of MMT systems is a combination of the transparency error in the steady and transition states. Combining them is an interesting topic for future work.

VIII. CONCLUSION AND FUTURE WORK

In this paper, we have presented an overview of relevant studies on model-mediated teleoperation (MMT) from the late 1980s to the present. The MMT method was developed to achieve both stability and transparency in the presence of communication delays. Based on a local model on the master side, which is a prediction of the remote environment, haptic feedback can be rendered locally without delay. According to the principle of the Smith Predictor, an MMT system can be both stable and transparent if the local model is an accurate approximation of the remote environment.

The most important challenge of MMT is the environment modeling. A precise and quickly converging model estimation algorithm is the key for designing an efficient MMT system. At present, the online estimation algorithms can deal with linear and non-linear environment models using only limited samples of slave motion and contact force information. For complex environment geometries, external 3D sensors can be employed to capture a precise description of the surface geometry. Besides the model estimation, other challenges such as data compression, model updating in the transition state, and slave control in the transition state are also discussed. Data compression reduces the communication load and avoids potential congestion in the network, especially for transmitting the model parameters of complex environments. Proper model updating and slave control schemes in the transition state ensure system stability when the local model on the master side is mismatched with the remote environment. The final goal of addressing these challenges is to ensure the stability of the slave-environment closed loop and the human local model closed loop, thus guaranteeing a stable and transparent teleoperation system.

In summary, it can be stated that the MMT approach has the benefit of being simultaneously stable and transparent for relatively simple environments. However, due to the limitations of existing online model-estimation algorithms, the MMT approach cannot work efficiently in complex or completely unknown environments. A table summarizing relevant studies on MMT can be found in the appendix.

Regarding future work, one idea is to develop an online modeling algorithm for deformable objects. This requires a sufficiently simple model whose parameters can be identified online and which can provide a sufficiently precise description of the deformable object. To be sufficiently simple, this model can be physically inaccurate, but should be able to provide a perceptually realistic haptic feedback.

| Paper Year | Environment modeling (Sec. III) | | | | Data transmission (Sec. IV) | | Model updating in transition state (Sec. V) | Slave control in transition state (Sec. VI) | | |
|---------------|---|------------------|-------------------------------|-------------------------------------|------------------------------------|---------------------------|---|---|--|--|
| | Adopted model | Model parameters | | Estimation method | Data type | Data reduction scheme | | | | |
| | | Geometry | Physical properties | | | | | | | |
| [21] /1989 | 1D, two-port model | - | H-matrix | analytical analysis | Torque & impedance (f,b) | - | - | - | | |
| [55] /1995 | Multi-DoF, mass-spring-damper | - | M, B, K | RLS | - | - | - | - | | |
| [35] /2003 | 1D, spring model | - | K | adaptation method (master side) | pos (f,b), force (b) | - | - | - | | |
| [29] /2004 | 3D, compliance model | - | compliance gains | pre-defined parameters | pos (f) | - | - | reference force | | |
| [32,33] /2005 | 3D, unknown model | neuron weights | online-trained neural network | pos (f), weights (b) | - | - | - | - | | |
| [38] /2006 | 1D, mass-spring-damper | P | I, B, K | laser rangefinder & SPRLS | vel (f), model data (b) | - | - | waiting strategy | | |
| [58] /2007 | 1D, mass-spring-damper | P | M, B, K | stereo camera & SALS (master side) | pos (f,b), force (b) | time-triggered estimation | - | - | | |
| [22] /2008 | 1D, rigid wall | P | - | force-based on-off contact detector | pos, vel, force (f) model data (b) | - | zero-energy injection | force-controlled while in contact | | |
| [27]/2008 | 1D, spring model | P | K | adaptation method | pos (f), model data (b) | - | - | - | | |
| [46]/2008 | 2D, plane | P, n | K, μ | Kalman filter-based | pos (f), model data (b) | event-triggered | - | - | | |
| [76] /2009 | 1D, spring model & human-trajectory model | - | K, T | RLS (master and slave sides) | pos (f,b), force (b) | - | - | - | | |
| [47] /2011 | 3D, smooth plane/sphere | P, n, R | K | block least square (master side) | pos (f), force (b) | perceptual deadband | - | - | | |
| [45] /2012 | 1D, rigid wall | P | - | force-based on-off contact detector | pos, vel, force (f) model data (b) | - | 1st-order lowpass filter | force-controlled while in contact | | |
| [23] /2012 | 2D, rough plane | P, n | - | stereo camera & force trajectory | pos, vel, force (f) model data (b) | - | - | force-controlled (normal direction) | | |
| [49] /2014 | 3D, complex surface | point cloud | K, μ | 3D sensor & block least squares | pos, vel, force (f) model data (b) | perceptual deadband | linear interpolation | relative tracking | | |

1D: one-dimensional. P: position. n: surface normal. R: sphere radius. M: mass. B: damping. K: stiffness. I: inertial.

μ : friction coefficient. T: movement duration. RLS: recursive least squares. SPRLS: self-perturbing recursive least squares. SALs: sliding-average least squares.

On the other hand, the use of more external sensors can improve the estimation accuracy of the model parameters. With the help of additional sensors, the model parameters, both geometric and physical properties, can be identified even before the slave gets into contact with the environment.

APPENDIX

A SUMMARY OF RELEVANT STUDIES ON MMT

A summary of relevant studies on MMT is shown in the previous page.

ACKNOWLEDGMENTS

The authors would like to thank the TUM English Writing Center and the TUM Graduate School for their help in improving the presentation of this paper.

REFERENCES

- [1] W. R. Ferrell and T. B. Sheridan, "Supervisory control of remote manipulation," *IEEE Spectr.*, vol. 4, no. 10, pp. 81–88, Oct. 1967.
- [2] A. Kron, G. Schmidt, B. Petzold, M. I. Zäh, P. Hinterseer, and E. Steinbach, "Disposal of explosive ordnances by use of a bimanual haptic telepresence system," in *Proc. IEEE Int. Conf. Robot. Autom.*, New Orleans, LA, USA, Apr. 2004, pp. 1968–1973.
- [3] T. B. Sheridan, "Space teleoperation through time delay: Review and prognosis," *IEEE Trans. Robot. Autom.*, vol. 9, no. 5, pp. 592–606, Oct. 1993.
- [4] L. F. Peñín, "Teleoperation with time delay—A survey and its issue in space robotics," in *Proc. 6th ESA Workshop Adv. Space Technol. Robot. Autom.*, Noordwijk, The Netherlands, 2000, pp. 1–8.
- [5] G. Hirzinger, B. Brunner, J. Dietrich, and J. Heindl, "ROTEX—the first remotely controlled robot in space," in *Proc. IEEE Int. Conf. Robot. Autom.*, San Diego, CA, USA, May 1994, pp. 2604–2611.
- [6] G. S. Guthart and J. Salisbury, Jr., "The Intuitive telesurgery system: Overview and application," in *Proc. IEEE Int. Conf. Robot. Autom.*, San Francisco, CA, USA, Apr. 2000, pp. 618–621.
- [7] H. Brandstädter, J. Schneider, and F. Freyberger, "Hardware and software components for a new Internet-based multimodal tele-control experiment with haptic sensation," in *Proc. EuroHaptics Conf.*, Munich, Germany, Jun. 2004, pp. 426–427.
- [8] A. El Saddik, "The potential of haptics technologies," *IEEE Instrum. Meas. Mag.*, vol. 10, no. 1, pp. 10–17, Feb. 2007.
- [9] A. Hamam, M. Eid, and A. El Saddik, "Effect of kinesthetic and tactile haptic feedback on the quality of experience of edutainment applications," *Multimedia Tools Appl.*, vol. 67, no. 2, pp. 455–472, Nov. 2013.
- [10] M. Eid, A. El Lssawi, and A. El Saddik, "Slingshot 3D: A synchronous haptic-audio-video game," *Multimedia Tools Appl.*, vol. 71, no. 3, pp. 1635–1649, Nov. 2012.
- [11] M. Eid, J. Cha, and A. El Saddik, "Admux: An adaptive multiplexer for haptic–audio–visual data communication," *IEEE Trans. Instrum. Meas.*, vol. 60, no. 1, pp. 21–31, Jan. 2011.
- [12] M. Buss and G. Schmidt, "Control problems in multi-modal telepresence systems," in *Advances in Control*, P. Frank, Ed. Berlin, Germany: Springer-Verlag, 1999, pp. 65–101.
- [13] D. A. Lawrence, "Stability and transparency in bilateral teleoperation," *IEEE Trans. Robot. Autom.*, vol. 9, no. 5, pp. 624–637, Oct. 1993.
- [14] G. Niemeyer and J.-J. E. Slotine, "Stable adaptive teleoperation," *IEEE J. Ocean. Eng.*, vol. 16, no. 1, pp. 152–162, Jan. 1991.
- [15] R. Anderson and M. W. Spong, "Bilateral control of teleoperators with time delay," *IEEE Trans. Autom. Control*, vol. 34, no. 5, pp. 494–501, May 1989.
- [16] D. Sun, F. Naghdy, and H. Du, "Application of wave-variable control to bilateral teleoperation systems: A survey," *Annu. Rev. Control*, vol. 38, no. 1, pp. 12–31, 2014.
- [17] B. Hannaford and J.-H. Ryu, "Time-domain passivity control of haptic interfaces," *IEEE Trans. Robot. Autom.*, vol. 18, no. 1, pp. 1–10, Feb. 2002.
- [18] J.-H. Ryu, "Bilateral control with time domain passivity approach under time-varying communication delay," in *Proc. 16th IEEE Int. Conf. Robot. Human Interact. Commun.*, Jeju, Korea, Aug. 2007, pp. 986–991.
- [19] J.-H. Ryu, J. Artigas, and C. Preusche, "A passive bilateral control scheme for a teleoperator with time-varying communication delay," *Mechatronics*, vol. 20, no. 7, pp. 812–823, Oct. 1994.
- [20] Y. Yokokohji and T. Yoshikawa, "Bilateral control of master-slave manipulators for ideal kinesthetic coupling-formulation and experiment," *IEEE Trans. Robot. Autom.*, vol. 10, no. 5, pp. 605–620, Oct. 1994.
- [21] P. F. Hokayem and M. W. Spong, "Bilateral teleoperation: An historical survey," *Automatica*, vol. 42, no. 12, pp. 2035–2057, Dec. 2006.
- [22] E. Nuño, L. Basañez, and R. Ortega, "Passivity-based control for bilateral teleoperation: A tutorial," *Automatica*, vol. 47, no. 3, pp. 485–495, Mar. 2011.
- [23] Z. Li, Y. Xia, and C.-Y. Su, *Intelligent Networked Teleoperation Control*. Berlin, Germany: Springer-Verlag, 2015.
- [24] R. W. Daniel and P. R. McAree, "Fundamental limits of performance for force reflecting teleoperation," *Int. J. Robot. Res.*, vol. 17, no. 8, pp. 811–830, 1998.
- [25] S. Hirche and M. Buss, "Human-oriented control for haptic teleoperation," *Proc. IEEE*, vol. 100, no. 3, pp. 623–647, Mar. 2012.
- [26] B. Hannaford, "A design framework for teleoperators with kinesthetic feedback," *IEEE Trans. Robot. Autom.*, vol. 5, no. 4, pp. 426–434, Aug. 1989.
- [27] P. Mitra and G. Niemeyer, "Model-mediated telemanipulation," *Int. J. Robot. Res.*, vol. 27, no. 2, pp. 253–262, Feb. 2008.
- [28] B. Willaert, J. Bohg, H. Van Brussel, and G. Niemeyer, "Towards multi-DOF model mediated teleoperation: Using vision to augment feedback," in *Proc. IEEE Int. Workshop HAVE*, Munich, Germany, Oct. 2012, pp. 25–31.
- [29] D. Feth, A. Peer, and M. Buss, "Incorporating human haptic interaction models into teleoperation systems," in *Proc. IEEE/RSJ Int. Conf. Intell. Robots Syst.*, Taipei, China, Oct. 2010, pp. 4257–4262.
- [30] C. Passenberg, A. Peer, and M. Buss, "A survey of environment-, operator-, and task-adapted controllers for teleoperation systems," *Mechatronics*, vol. 20, no. 7, pp. 787–801, Oct. 2010.
- [31] C. Passenberg, A. Peer, and M. Buss, "Model-mediated teleoperation for multi-operator multi-robot systems," in *Proc. IEEE/RSJ Int. Conf. Intell. Robots Syst.*, Taipei, China, Oct. 2010, pp. 4263–4268.
- [32] P. Arcara and C. Melchiorri, "Control schemes for teleoperation with time delay: A comparative study," *Robot. Auto. Syst.*, vol. 38, no. 1, pp. 49–64, Jan. 2002.
- [33] C. Tzafestas, S. Velanas, and G. Fakiridis, "Adaptive impedance control in haptic teleoperation to improve transparency under time-delay," in *Proc. IEEE Int. Conf. Robot. Autom.*, Pasadena, CA, USA, May 2008, pp. 212–219.
- [34] S. V. Velanas and C. S. Tzafestas, "Human telehaptic perception of stiffness using an adaptive impedance reflection bilateral teleoperation control scheme," in *Proc. IEEE Int. Symp. Robot Human Interact. Commun.*, Viareggio, Italy, Sep. 2010, pp. 21–26.
- [35] S. V. Velanas and C. S. Tzafestas, "Model-mediated telehaptic perception of delayed curvature," in *Proc. IEEE Int. Symp. Robot Human Interact. Commun.*, Paris, France, Sep. 2012, pp. 941–947.
- [36] C. Tzafestas and S. Velanas, "Telehaptic perception of delayed stiffness using adaptive impedance control: Experimental psychophysical analysis," *Presence Teleoper. Virtual Environ.*, vol. 22, no. 4, pp. 323–344, 2013.
- [37] J. Smisek, R. M. van Paassen, and A. Schiele, "Naturally-transitioning rate-to-force controller robust to time delay by model-mediated teleoperation," in *Proc. IEEE Int. Conf. Syst., Man, Cybern.*, Oct. 2015.
- [38] L. J. Love and W. J. Book, "Force reflecting teleoperation with adaptive impedance control," *IEEE Trans. Syst., Man, Cybern. B, Cybern.*, vol. 34, no. 1, pp. 159–165, Feb. 2004.
- [39] W.-K. Yoon et al., "Model-based space robot teleoperation of ETS-VII manipulator," *IEEE Trans. Robot. Autom.*, vol. 20, no. 3, pp. 602–612, Jun. 2004.
- [40] T. Kotoku, "A predictive display with force feedback and its application to remote manipulation system with transmission time delay," in *Proc. IEEE/RSJ Int. Conf. Intell. Robots Syst.*, Jul. 1992, pp. 239–246.
- [41] J.-Q. Huang and F. L. Lewis, "Neural-network predictive control for nonlinear dynamic systems with time-delay," *IEEE Trans. Neural Netw.*, vol. 14, no. 2, pp. 377–389, Feb. 2003.
- [42] A. C. Smith and K. Hashrudi-Zaad, "Adaptive teleoperation using neural network-based predictive control," in *Proc. IEEE Int. Conf. Control Appl.*, Toronto, ON, USA, Aug. 2005, pp. 1269–1274.

- [43] A. C. Smith and K. Hashtrudi-Zaad, "Neural network-based teleoperation using Smith predictors," in *Proc. IEEE Int. Conf. Mechatronics Autom.*, Niagara Falls, ON, Canada, Jul. 2005, pp. 1654–1659.
- [44] J. Sheng and M. W. Spong, "Model predictive control for bilateral teleoperation systems with time delays," in *Proc. Can. Conf. Elect. Comput. Eng.*, May 2004, pp. 1877–1880.
- [45] K. B. Fite, M. Goldfarb, and A. Rubio, "Transparent telemanipulation in the presence of time delay," in *Proc. IEEE/ASME Int. Conf. Adv. Intell. Mechatronics*, Jul. 2003, pp. 254–259.
- [46] A. Alfi and M. Farrokhi, "A simple structure for bilateral transparent teleoperation systems with time delay," *J. Dyn. Syst., Meas., Control*, vol. 130, no. 4, p. 044502, Jul. 2008.
- [47] A. Alfi and M. Farrokhi, "Force reflecting bilateral control of master-slave systems in teleoperation," *J. Intell. Robot. Syst.*, vol. 52, no. 2, pp. 209–232, Mar. 2008.
- [48] S. Clarke, G. Schillhuber, M. F. Zaeh, and H. Ulbrich, "Prediction-based methods for teleoperation across delayed networks," *Multimedia Syst.*, vol. 13, no. 4, pp. 253–261, Jan. 2008.
- [49] M. V. Noyes and T. B. Sheridan, "A novel predictor for telemanipulation through a time delay," in *Proc. Annu. Conf. Manual Control*, Moffett Field, CA, USA, 1984.
- [50] F. Mobasser and K. Hashtrudi-Zaad, "Predictive teleoperation using laser rangefinder," in *Proc. Can. Conf. Elect. Comput. Eng.*, Ottawa, ON, Canada, May 2006, pp. 1279–1282.
- [51] O. J. M. Smith, "Close control of loops with dead time," *Chem. Eng. Prog.*, vol. 53, no. 5, pp. 217–219, 1957.
- [52] A. K. Bejczy, W. S. Kim, and S. C. Venema, "The phantom robot: Predictive displays for teleoperation with time delay," in *Proc. IEEE Int. Conf. Robot. Autom.*, Cincinnati, OH, USA, May 1990, pp. 546–551.
- [53] A. K. Bejczy and W. S. Kim, "Predictive displays and shared compliance control for time-delayed telemanipulation," in *Proc. Int. Conf. IROS*, Ibaraki, Japan, Jul. 1990, pp. 407–412.
- [54] T. Burkert, J. Leupold, and G. Passig, "A photorealistic predictive display," *Presence, Teleoper. Virtual Environ.*, vol. 13, no. 1, pp. 22–43, Feb. 2004.
- [55] F. T. Buzan and T. B. Sheridan, "A model-based predictive operator aid for telemanipulators with time delay," in *Proc. IEEE Int. Conf. Syst., Man Cybern.*, Cambridge, MA, USA, Nov. 1989, pp. 138–143.
- [56] C. Zhao, "Real time haptic simulation of deformable bodies," M.S. thesis, Inst. Appl. Mech., Faculty Mech. Eng., Tech. Univ. München, München, Germany, 2010.
- [57] B. Willaert, H. Van Brussel, and G. Niemeyer, "Stability of model-mediated teleoperation: Discussion and experiments," in *Proc. Eurohaptics*, Tampere, Finland, Jun. 2012, pp. 625–636.
- [58] D. Verschueren, J. Swevers, H. Bruyninckx, and J. De Schutter, "Online identification of contact dynamics in the presence of geometric uncertainties," in *Proc. IEEE Int. Conf. Robot. Autom.*, Pasadena, CA, USA, May 2008, pp. 851–856.
- [59] X. Xu, J. Kammerl, R. Chaudhari, and E. Steinbach, "Hybrid signal-based and geometry-based prediction for haptic data reduction," in *Proc. IEEE Int. Workshop HAVE*, Hebei, China, Oct. 2011, pp. 68–73.
- [60] X. Xu, B. Cizmeci, and E. Steinbach, "Point-cloud-based model-mediated teleoperation," in *Proc. IEEE Int. Workshop HAVE*, Istanbul, Turkey, Oct. 2013, pp. 69–74.
- [61] X. Xu, B. Cizmeci, A. Al-Nuaimi, and E. Steinbach, "Point cloud-based model-mediated teleoperation with dynamic and perception-based model updating," *IEEE Trans. Instrum. Meas.*, vol. 63, no. 11, pp. 2558–2569, May 2014.
- [62] J. E. Colgate and G. G. Schenkel, "Passivity of a class of sampled-data systems: Application to haptic interfaces," *J. Robot. Syst.*, vol. 14, no. 1, pp. 37–47, Jan. 1997.
- [63] M. Mahvash and V. Hayward, "High-fidelity passive force-reflecting virtual environments," *IEEE Trans. Robot.*, vol. 21, no. 1, pp. 38–46, Feb. 2005.
- [64] J. J. Abbott and A. M. Okamura, "Effects of position quantization and sampling rate on virtual-wall passivity," *IEEE Trans. Robot.*, vol. 21, no. 5, pp. 952–964, Oct. 2005.
- [65] N. Diolaiti, G. Niemeyer, F. Barbagli, and J. K. Salisbury, "Stability of haptic rendering: Discretization, quantization, time delay, and Coulomb effects," *IEEE Trans. Robot.*, vol. 22, no. 2, pp. 256–268, Apr. 2006.
- [66] N. Hogan, "Impedance control: An approach to manipulation," in *Proc. Amer. Control Conf.*, San Diego, CA, USA, Jun. 1984, pp. 304–313.
- [67] L. J. Love and W. J. Book, "Environment estimation for enhanced impedance control," in *Proc. IEEE Int. Conf. Robot. Autom.*, Nagoya, Japan, May 1995, pp. 1854–1859.
- [68] H. Seraji, D. Lim, and R. Steele, "Experiments in contact control," *J. Robot. Syst.*, vol. 13, no. 2, pp. 53–73, Feb. 1996.
- [69] H. Seraji and R. Colbaugh, "Force tracking in impedance control," *Int. J. Robot. Res.*, vol. 16, no. 1, pp. 97–117, Feb. 1997.
- [70] H. Li and A. Song, "Virtual-environment modeling and correction for force-reflecting teleoperation with time delay," *IEEE Trans. Ind. Electron.*, vol. 54, no. 2, pp. 1227–1233, Apr. 2007.
- [71] A. Haddadi and K. Hashtrudi-Zaad, "Online contact impedance identification for robotic systems," in *Proc. IEEE/RSJ Int. Conf. IROS*, Nice, France, Sep. 2008, pp. 974–980.
- [72] D. Erickson, M. Weber, and I. Sharf, "Contact stiffness and damping estimation for robotic systems," *Int. J. Robot. Res.*, vol. 22, no. 1, pp. 41–57, Jan. 2003.
- [73] K. Hunt and F. Crossley, "Coefficient of restitution interpreted as damping in vibroimpact," *J. Appl. Mech.*, vol. 42, no. 2, pp. 440–445, Jun. 1975.
- [74] D. W. Marhefka and D. E. Orin, "A compliant contact model with nonlinear damping for simulation of robotic systems," *IEEE Trans. Syst., Man, Cybern. A, Syst., Humans*, vol. 29, no. 6, pp. 566–572, Nov. 1999.
- [75] N. Diolaiti, C. Melchiorri, and S. Stramigioli, "Contact impedance estimation for robotic systems," *IEEE Trans. Robot.*, vol. 21, no. 5, pp. 925–935, Oct. 2005.
- [76] A. Haddadi and K. Hashtrudi-Zaad, "A new method for online parameter estimation of Hunt–Crossley environment dynamic models," in *Proc. IEEE/RSJ Int. Conf. Intell. Robots Syst.*, Nice, France, Sep. 2008.
- [77] A. Achhammer, C. Weber, A. Peer, and M. Buss, "Improvement of model-mediated teleoperation using a new hybrid environment estimation technique," in *Proc. IEEE Int. Conf. Robot. Autom.*, Anchorage, AK, USA, May 2010, pp. 5358–5363.
- [78] D.-J. Park and B.-E. Jun, "Selfperturbing recursive least squares algorithm with fast tracking capability," *Electron. Lett.*, vol. 28, no. 65, pp. 558–559, Mar. 1992.
- [79] J. Funda and R. P. Paul, "Efficient control of a robotic system for time-delayed environments," in *Proc. 5th Int. Conf. Adv. Robot.*, Pisa, Italy, Jun. 1991, pp. 219–224.
- [80] R. C. Winck et al., "Time-delayed teleoperation for interaction with moving objects in space," in *Proc. IEEE Int. Conf. Robot. Autom.*, Hong Kong, May/Jun. 2014, pp. 5952–5958.
- [81] X. Xu, S. Chen, and E. Steinbach, "Model-mediated teleoperation for movable objects: Dynamics modeling and packet rate reduction," in *Proc. 14th IEEE Int. Symp. Haptic Audio-Vis. Environ. Games*, Ottawa, ON, Canada, Oct. 2015, pp. 1–6.
- [82] D. Terzopoulos, J. Platt, A. Barr, and K. Fleischer, "Elastically deformable models," *SIGGRAPH Comput. Graph.*, vol. 21, no. 4, pp. 205–214, Jul. 1987.
- [83] B. A. Lloyd, G. Székely, and M. Harders, "Identification of spring parameters for deformable object simulation," *IEEE Trans. Vis. Comput. Graphics*, vol. 13, no. 5, pp. 1081–1094, Sep. 2007.
- [84] H. Delingette, "Toward realistic soft-tissue modeling in medical simulation," *Proc. IEEE*, vol. 86, no. 3, pp. 512–523, Mar. 1998.
- [85] X. Xu and E. Steinbach, "Towards real-time modeling and haptic rendering of deformable objects for point cloud-based model-mediated teleoperation," in *Proc. IEEE Int. Conf. ICME Workshops (Hot3D)*, Chengdu, China, Jul. 2014, pp. 1–6.
- [86] Z. Li, Y. Xia, D. Wang, D.-H. Zhai, C.-Y. Su, and X. Zhao, "Neural network-based control of networked trilateral teleoperation with geometrically unknown constraints," *IEEE Trans. Cybern.*, May 2015.
- [87] Z. Li and Y. Xia, "Adaptive neural network control of bilateral teleoperation with unsymmetrical stochastic delays and unmodeled dynamics," *Int. J. Robust Nonlinear Control*, vol. 24, no. 11, pp. 1628–1652, Jul. 2014.
- [88] Z. Li, Y. Xia, and F. Sun, "Adaptive fuzzy control for multilateral cooperative teleoperation of multiple robotic manipulators under random network-induced delays," *IEEE Trans. Fuzzy Syst.*, vol. 22, no. 2, pp. 437–450, Apr. 2014.
- [89] K. J. Astrom and T. Bohlin, *Theory of Self-Adaptive Control Systems*, P. H. Hammond, Ed. New York, NY, USA: Plenum, 1966, p. 96.
- [90] K. S. Narendra and A. M. Annaswamy, "Persistent excitation in adaptive systems," *Int. J. Control.*, vol. 45, no. 1, pp. 127–160, 1987.
- [91] P. Ioannou and B. Fidan, *Adaptive Control Tutorial*. Philadelphia, PA, USA: SIAM, 2006.

- [92] J. G. Gonzalez, E. A. Heredia, T. Rahman, K. E. Barner, and G. R. Arce, "Customized optimal filter for eliminating operator's tremor," *Proc. SPIE 2590, Telemanipulator and Telepresence Technologies II*, pp. 131–142, Dec. 1995.
- [93] C. Weber, V. Nitsch, U. Unterhinninghofen, B. Färber, and M. Buss, "Position and force augmentation in a telepresence system and their effects on perceived realism," in *Proc. 3rd Joint EuroHaptics Conf. Symp. Haptic Interfaces Virtual Environ. Teleoper. Syst.*, Salt Lake City, UT, USA, Mar. 2009, pp. 226–231.
- [94] P. A. Prekopiou, S. G. Tzafestas, and W. S. Harwin, "Towards variable-time-delays-robust telemanipulation through master state prediction," in *Proc. IEEE/ASME Int. Conf. Adv. Intell. Mechatronics*, Atlanta, GA, USA, Sep. 1999, pp. 305–310.
- [95] I. Belghit, B. Hennion, and A. Guerraz, "Predictive algorithms for distant touching," in *Proc. EuroHaptics*, 2002, p. 55.
- [96] T. Flash and N. Hogan, "The coordination of arm movements: An experimentally confirmed mathematical model," *J. Neurosci.*, vol. 5, no. 7, pp. 1688–1703, Jan. 1985.
- [97] P. R. McAree and R. W. Daniel, "Stabilizing impacts in force-reflecting teleoperation using distance-to-impact estimates," *Int. J. Robot. Res.*, vol. 19, no. 4, pp. 349–364, Apr. 2000.
- [98] Z. Li and C.-Y. Su, "Neural-adaptive control of single-master–multiple-slaves teleoperation for coordinated multiple mobile manipulators with time-varying communication delays and input uncertainties," *IEEE Trans. Neural Netw. Learn. Syst.*, vol. 24, no. 9, pp. 1400–1413, Sep. 2013.
- [99] J. E. Colgate and J. M. Brown, "Factors affecting the Z-width of a haptic display," in *Proc. IEEE Int. Conf. Robot. Autom.*, San Diego, CA, USA, May 1994, pp. 3205–3210.
- [100] H. Z. Tan, M. A. Srinivasan, B. Eberman, and B. Cheng, "Human factors for the design of force-reflecting haptic interfaces," in *Proc. 3rd Annu. Symp. Haptic Interfaces Virtual Environ. Teleoper. Syst.*, 1994, pp. 1–7.
- [101] P. Hinterseer, E. Steinbach, S. Hirche, and M. Buss, "A novel, psychophysically motivated transmission approach for haptic data streams in telepresence and teleaction systems," in *Proc. IEEE Int. Conf. Acoust., Speech, Signal Process.*, Mar. 2005, pp. II/1097–II/1100.
- [102] P. Hinterseer, S. Hirche, S. Chaudhuri, and E. Steinbach, "Perception-based data reduction and transmission of haptic data in telepresence and teleaction systems," *IEEE Trans. Signal Process.*, vol. 56, no. 2, pp. 588–597, Feb. 2008.
- [103] E. Steinbach, S. Hirche, J. Kammerl, I. Vittorias, and R. Chaudhari, "Haptic data compression and communication," *IEEE Signal Process. Mag.*, vol. 28, no. 1, pp. 87–96, Jan. 2011.
- [104] S. Hirche, P. Hinterseer, E. Steinbach, and M. Buss, "Transparent data reduction in networked telepresence and teleaction systems. Part I: Communication without time delay," *Presence, Teleoper. Virtual Environ.*, vol. 16, no. 5, pp. 523–531, Jan. 2007.
- [105] S. Hirche and M. Buss, "Transparent data reduction in networked telepresence and teleaction systems. Part II: Time-delayed communication," *Presence, Teleoper. Virtual Environ.*, vol. 16, no. 5, pp. 532–542, Jan. 2007.
- [106] I. Vittorias, J. Kammerl, S. Hirche, and E. Steinbach, "Perceptual coding of haptic data in time-delayed teleoperation," in *Proc. World Haptics Conf.*, Salt Lake City, UT, USA, Mar. 2009, pp. 208–213.
- [107] X. Xu, B. Cizmeci, C. Schuwerk, and E. Steinbach, "Haptic data reduction for time-delayed teleoperation using the time domain passivity approach," in *Proc. IEEE World Haptics Conf.*, Chicago, IL, USA, Jun. 2015, pp. 512–518.
- [108] J. Kammerl, N. Blodow, R. B. Rusu, S. Gedikli, M. Beetz, and E. Steinbach, "Real-time compression of point cloud streams," in *Proc. IEEE Int. Conf. Robot. Autom. (ICRA)*, Saint Paul, MN, USA, May 2012, pp. 778–785.
- [109] C. B. Zilles and J. K. Salisbury, "A constraint-based god-object method for haptic display," in *Proc. IEEE/RSJ Int. Conf. Intell. Robots Syst.*, Pittsburgh, PA, USA, Aug. 1995, pp. 146–151.
- [110] F. Ryden, S. N. Kosari, and H. J. Chizeck, "Proxy method for fast haptic rendering from time varying point clouds," in *Proc. IEEE/RSJ Int. Conf. Intell. Robots Syst.*, San Francisco, CA, USA, Sep. 2011, pp. 2614–2619.
- [111] F. Ryden and H. J. Chizeck, "A proxy method for real-time 3-DOF haptic rendering of streaming point cloud data," *IEEE Trans. Haptics*, vol. 6, no. 3, pp. 257–267, Jul./Sep. 2013.
- [112] Z. C. Marton, R. B. Rusu, and M. Beetz, "On fast surface reconstruction methods for large and noisy point clouds," in *Proc. IEEE Int. Conf. Robot. Autom. (ICRA)*, Kobe, Japan, May 2009, pp. 3218–3223.
- [113] P. Mitra, D. Gentry, and G. Niemeyer, "User Perception and Preference in Model Mediated Telemanipulation," in *Proc. IEEE World Haptics Conf.*, Tsukuba, Japan, Mar. 2007, pp. 268–273.
- [114] X. Xu, C. Schuwerk, and E. Steinbach, "Passivity-based model updating for model-mediated teleoperation," in *Proc. IEEE Int. Conf. Multimedia Expo Workshops*, Turin, Italy, Jun./Jul. 2015, pp. 1–6.
- [115] I. S. MacKenzie and C. Ware, "Lag as a determinant of human performance in interactive systems," in *Proc. INTERACT CHI Conf. Human Factors Comput. Syst.*, New York, NY, USA, Apr. 1993, pp. 488–493.
- [116] I. M. Vogels, "Detection of temporal delays in visual-haptic interfaces," *Human Factors, J. Human Factors Ergonom. Soc.*, vol. 46, no. 1, pp. 118–134, 2004.
- [117] C. Jay and R. Hubbold, "Delayed visual and haptic feedback in a reciprocal tapping task," in *Proc. IEEE World Haptics Conf.*, Mar. 2005, pp. 655–656.
- [118] X. Xu, G. Pagetti, and E. Steinbach, "Dynamic model displacement for model-mediated teleoperation," in *Proc. IEEE World Haptics Conf.*, Daejeon, Korea, Apr. 2013, pp. 313–318.
- [119] R. C. Winck and A. M. Okamura, "Model-mediated teleoperation with predictive models and relative tracking," in *Proc. Dyn. Syst. Control Conf.*, Stanford, CA, USA, Oct. 2013, p. V002T26A003.



XIAO XU (M'11) received the B.Sc. degree in information engineering from Shanghai Jiao Tong University, China, in 2008, and the M.Sc. degree in information engineering from the Technische Universität München, Germany, in 2011. He joined the Media Technology Group, Technische Universität München, in 2011, where he is currently a member of the Research Staff. His current research interests are in the field of perceptual coding of haptic data streams with stability ensuring control architectures and the model-mediated telemanipulation.



BURAK CIZMECI (M'11) received the B.Sc. degree in electronics engineering in 2007, and the B.Sc. degree in computer engineering and the M.Sc. degree in electronics engineering from Isik University, Istanbul, Turkey, in 2008 and 2009, respectively. He was a Teaching Assistant with the Department of Electronics Engineering, Isik University, from 2007 to 2010. During his master's studies, he actively worked on video analysis, coding, de-noising, frame rate up-conversion, and superresolution. In 2010, he joined the Media Technology Group, Technische Universität München, Germany, to pursue the Ph.D. degree as a German Academic Exchange Service Scholarship Holder. He is currently with the European Research Council supported project called Haptic Signal Processing and Communication. His research focuses on the real-time transmission of audio, video, and haptic signals for telepresence and teleaction systems. More specifically, he develops communication protocols and signal processing solutions for multimodal signal transmission.



CLEMENS SCHUWERK (M'11) received the degree in electrical engineering from the Technische Universität München (TUM), Germany, and the University of Edinburgh, Scotland, and the Dipl.-Ing. (Univ.) degree in electrical engineering from TUM, in 2010. He joined the Chair of Media Technology, TUM, in 2011, where he is currently a member of the Research Staff. His current research interests lie in the area of haptic data communication and signal processing, especially in shared haptic virtual environments. In 2014, he received the Best Poster Award for the paper Delay Compensation in Shared Haptic Virtual Environments at the IEEE Haptics Symposium in Houston.



ECKEHARD STEINBACH (M'96–SM'08–F'15) received the degrees in electrical engineering from the University of Karlsruhe, Germany, the University of Essex, U.K., and ESIEE, Paris, and the Engineering Doctorate degree in 1999. From 1994 to 2000, he was a member of the Research Staff with the Image Communication Group, University of Erlangen–Nuremberg, Germany. From 2000 to 2001, he was a Post-Doctoral Fellow with the Information Systems Laboratory, Stanford University. In 2002, he joined the Department of Electrical and Computer Engineering, Technische Universität München, Germany, where he is currently a Full Professor of Media Technology. His current research interests are in the area of audio–visual–haptic information processing and communication, and networked and interactive multimedia systems.

• • •